

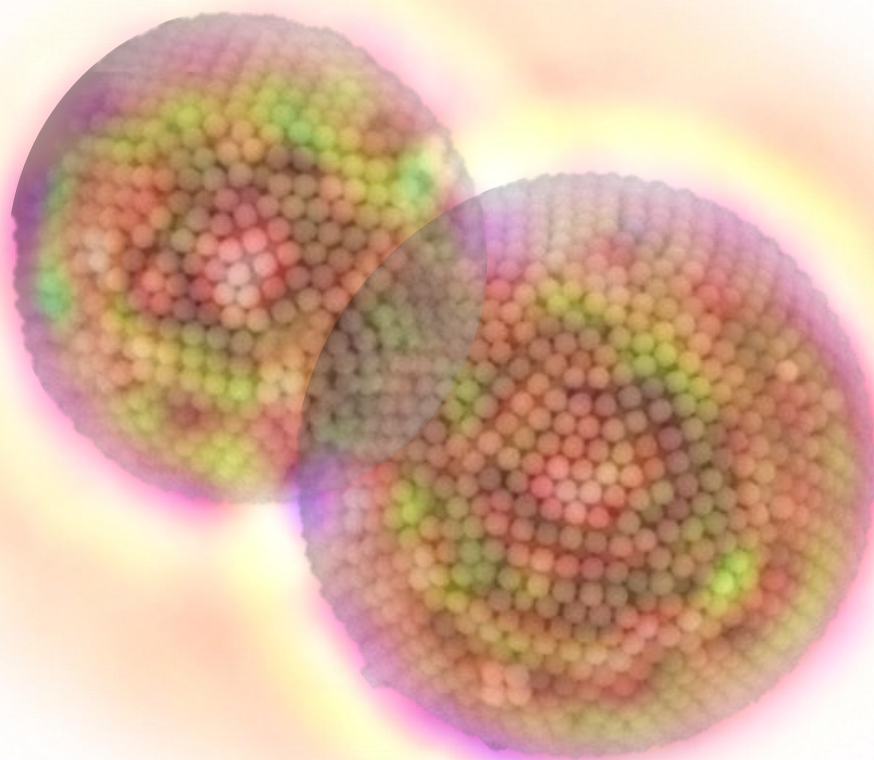
Master Project Report

# SELF-ASSEMBLY OF TITANIA SUPRAPARTICLES

Sofie M. Castelein BSc

Master Bio Inspired Innovation

October 8<sup>st</sup>, 2021



*Supervisors:*

Prof. Dr. Alfons van Blaaderen  
Dr. Arnout Imhof

*Daily Supervisor:*

Zahra Peimanifard MSc

Soft Condensed Matter Group  
Debye Institute for Nanomaterials Science  
Utrecht University, The Netherlands  
[www.colloid.nl](http://www.colloid.nl)

*“The whole is more than the sum of its parts”*

-Aristotle

Cover: Colour enhanced overlay of icosahedral titania supraparticles SEM and optical microscope images

# 1 Abstract

Titania is one of the most abundant and biocompatible compounds on our planet while also possessing strong optical properties. These optical properties can be further enhanced and manipulated by altering size, shape and structure of the titania. In this project, monodisperse amorphous titania colloids with a polydispersity of 6% and an average diameter of 438 nm were successfully synthesized through a sol-gel method. In this form the colloids displayed iridescent colours, after self-assembly (SA) into colloidal crystals. After silica coating of these titania colloids, stable titania-silica composites were formed with a polydispersity of only 3% and an average diameter of 421 nm, still exhibiting iridescence after SA. These composites were used to successfully form onion shaped and icosahedral photonic supraparticles with diameters ranging between 3 and 30  $\mu\text{m}$  through evaporation induced self-assembly. Especially the icosahedral supraparticles showed bright and patterned colouring upon illumination. The titania-silica composites were also functionalised with octadecyltrimethoxysilane (OTMOS) and dispersed in nonpolar solvents. These colloids had a polydispersity of 4% and an average diameter of 506 nm, they did not show iridescence and formed only partially crystalline supraparticles with diameters ranging between 4 and 20  $\mu\text{m}$ .

The strong display of colours in our synthesized photonic supraparticles shows great promise for future applications in nanophotonics, photocatalysis and structural colouring. However, many parameters used in the experiments are not yet optimized, such as the speed of SA, or fully understood, decreasing reproducibility of the experiments and control over the self-assembly of the supraparticles. Future research should focus on these parameters so that consistent photonic supraparticles can be synthesized.

# Table of contents

<b>1</b>	<b>ABSTRACT</b> .....	<b>3</b>
<b>2</b>	<b>INTRODUCTION</b> .....	<b>5</b>
<b>3</b>	<b>THEORETICAL BACKGROUND</b> .....	<b>8</b>
3.1	TITANIA COLLOID SYNTHESIS BY SOL-GEL METHOD .....	8
3.2	STÖBER METHOD .....	10
3.3	FUNCTIONALISATION .....	10
3.4	SELF-ASSEMBLY THROUGH SPHERICAL CONFINEMENT .....	11
<b>4</b>	<b>RESULTS AND DISCUSSION</b> .....	<b>13</b>
4.1	TITANIA COLLOID SYNTHESIS .....	13
4.1.1	<i>Titania size experiments</i> .....	13
4.1.2	<i>Condensation experiments</i> .....	13
4.2	STÖBER SILICA COATING .....	15
4.2.1	<i>FTTC functionalisation</i> .....	15
4.2.2	<i>Single silica layer</i> .....	16
4.4	SUPRAPARTICLES .....	19
4.4.1	<i>Water in oil</i> .....	19
4.4.2	<i>Oil in water</i> .....	24
<b>5</b>	<b>CONCLUSION AND OUTLOOK</b> .....	<b>27</b>
<b>6</b>	<b>MATERIALS AND METHODS</b> .....	<b>29</b>
6.1	CHEMICALS AND MATERIALS .....	29
6.2	AMORPHOUS TITANIA COLLOID SYNTHESIS .....	29
6.2.1	<i>Titania condensation experiments</i> .....	29
6.3	SILICA COATING OF THE TITANIA COLLOIDS <sup>43</sup> .....	30
6.3.1	<i>Fluorescein isothiocyanate (FITC) functionalisation</i> .....	30
6.4	OCTADECYLTRIMETHOXY-SILANE (OTMOS) FUNCTIONALISATION <sup>43</sup> .....	31
6.5	SUPRAPARTICLE FORMATION .....	31
6.5.1	<i>Water in oil emulsion<sup>2</sup></i> .....	31
6.5.2	<i>Oil in water emulsion<sup>44</sup></i> .....	31
6.6	MICROSCOPES USED .....	31
6.6.1	<i>Confocal imaging</i> .....	32
6.6.2	<i>Scanning Electron Microscopy (SEM) imaging</i> .....	32
6.6.3	<i>Transmission Electron Microscopy (TEM) and Energy Dispersive X-Ray (EDX) imaging</i> .....	32
6.7	POLYDISPERSITY CALCULATION .....	32
<b>7</b>	<b>ACKNOWLEDGEMENTS</b> .....	<b>33</b>
<b>8</b>	<b>BIBLIOGRAPHY</b> .....	<b>34</b>
<b>9</b>	<b>LAYMEN'S SUMMARY</b> .....	<b>37</b>
<b>10</b>	<b>APPENDICES</b> .....	<b>38</b>
10.1	TITANIA COLLOIDS DISSOLVED IN ETHANOL .....	38
10.2	EDX TITANIA-SILICA COMPOSITES .....	39
10.3	EDX OTMOS COATED TITANIA-SILICA COMPOSITES .....	41
10.4	SYNTHESIS SET-UPS .....	43
10.5	POLYDISPERSITY PYTHON CODE FROM MAARTEN BRANSEN .....	45

## 2 Introduction

The 21<sup>st</sup> century comes with many challenges. It has become apparent that resources are finite and that global warming can no longer be ignored. To overcome these challenges we have to be resourceful and creative in our new technologies. One of the solutions to create more sustainable and environmentally friendly materials is to take structure and the type of material into account. We became aware of the importance of structure through the many examples in nature. A complex structure can be just as strong while at the same time less material costly than just a simple structure. A beautiful example of this phenomenon is provided by the architect Michael Pawlyn<sup>1</sup> who in a simple sketch shows that a pillar of equal strength can be created by using only two percent of the original amount of material (figure 2.1<sup>3</sup>).

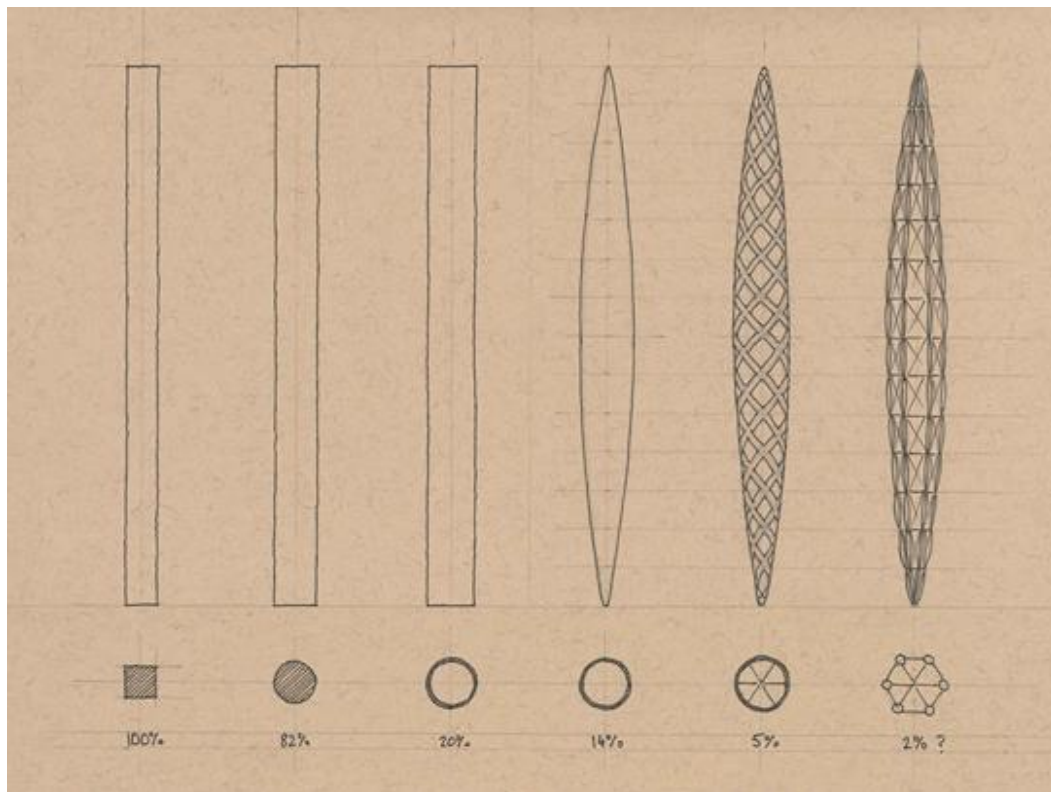


**Figure 2.1:** Sketch by Michael Pawlyn, one of the first architect using bio-mimicry in his designs, showing the benefit of structure over material. Sketch originating from biomimicry KTH.

In another biological example we see the importance of structure at the nanoscale, take for instance the wings of a *Morpho* butterfly. The surface of these wings consists of a nanostructure acting as a photonic crystal. Interference patterns cause incident light to reflect in a blue or green iridescent colour, even though the wings themselves are not actually this colour. This effect is called structural colouring and inspired many researchers to mimic these effects<sup>3-5</sup>. It is also a prime example that shows that new material properties can arise solely through structure.

In this project we make use of the structure in photonic crystals to enhance the optical properties of the metal oxide, titania ( $\text{TiO}_2$ ).

Titania is one of the most abundant compounds on our planet, while also being biocompatible. It occurs in nature in three different crystalline phases: rutile, anatase and brookite. Because of its many interesting properties such as a high thermal and chemical stability, unique photonic and chemical characteristics and suitable band position, titania is a popularly studied material among scientists<sup>6</sup>. It is commonly used in many products such as inorganic pigments, UV sunscreens, medical implants and cosmetics. Recently,

titania is also used in other applications including optoelectronics, semiconductors, catalysis, photovoltaics, batteries, fuel cells, smart windows, and self-cleaning and antifogging surfaces<sup>7</sup>.

In this study we mainly focus on the optical properties of titania. Normally, titania nanomaterials are transparent in the visible light region. But it is possible to improve the optical sensitivity and activity of the titania materials to the visible light spectrum. Thereby improving the light harvesting and conversion efficiency of solar energy by utilizing a larger fraction of the sun's light spectrum<sup>8</sup>.

This promising photocatalyst is expected to help solve many environmental and pollution challenges. Mainly through effective utilization of solar energy by implementation in photovoltaic and water-splitting devices, and hereby alleviating the energy crisis<sup>8</sup>. Since the most interesting properties occur on the nanoscale there have been many studies on nanostructured titania<sup>6,8-10</sup>. Of all the studied morphologies, spherical colloids below a micrometre in diameter are one of the most important ones. Spheres are an isotropic structure, meaning that the properties are generally uniform. Together with their monodispersity, self-assembling nature, close packing and enhanced light harvesting properties, titania colloids are of significant value in novel texture design and photochemical applications<sup>6</sup>. The first spherical titania colloids were reported by Matijević et al. in 1977<sup>11</sup>. Their synthesis was based on a forced precipitation method and was later significantly improved by sol-gel chemistry and the use of titania alkoxides. Other methods to synthesize titania colloids include aqueous methods like the hydrothermal method, nonaqueous methods such as the solvothermal and nonhydrolytic method but there are also hard- and soft templated techniques.

The sol-gel method is widely used for synthesizing colloids. It is a quick and easy method where a sol, the solution of the precursor compounds, is transformed into a gel, where the precursor after a series of chemical reactions has formed a metal-oxygen bond network within a continuous liquid phase. Colloids formed with this method are usually amorphous or poorly crystalline because the reaction is performed at room temperature. Therefore, it is often necessary to perform some kind of thermal treatment of the colloids to increase their stability and crystallinity. Because this method uses water the hydrolysis and condensation reactions occur fast and shape, size and dispersibility of the colloids is difficult to control.

Hydrothermal methods require few steps and only several important factors such as reaction time, pH, temperature, mineralizers and stirring to control the morphology and phase of the crystallites. Bases such as ammonia or alkaline hydroxides are used to form a titanium hydroxide intermediate, which is then dehydrated to titania under the applied hydrothermal reaction conditions at relatively high temperatures, typically between 150 and 250 °C. The resulting colloids have generally improved crystallinity compared to sol-gel methods but properties such as solubility, uniformity and processability are variable and difficult to control. Chemseddine and Moritz (1999)<sup>12</sup> were one of the firsts to use this method to manipulate the titania crystal shape and many have since followed to try to improve the controllability of this method with different additives<sup>13-15</sup>.

In nonaqueous methods, water is not added as one of the reactants. The proposed advantage of this is that the reaction time is better controlled since without the presence of water the hydrolysis and condensation reactions occur at a much more sedate pace. The solvothermal method is very similar to the hydrothermal method only without water as the primary solvent, making chemicals that are insoluble in aqueous-based mixtures now also available for use. This method quickly proved that the shape and size of the titania colloids is largely dependent on the choice of solvent<sup>16</sup>. The nonhydrolytic method uses surfactant-assisted processes to modulate the growth and formation of the titania colloids. The advantage of this method is that with the right choice of surfactant, the reactivity of the titania precursor can be further modulated. The additional control over the formation of the titania network also allows to controllably synthesize larger titania structures<sup>17</sup>.

Templated techniques combine the other methods with seeded growth of the titania colloid into or on top of a template, thereby controlling the morphology of the colloids. There is a distinction between hard and soft templates. Where hard templates<sup>18</sup> typically consist of rigid structures formed by inorganic

colloids or polymer beads and soft templates<sup>19</sup> are more flexible structures formed by microemulsions, proteins or micelles.

In this project we make use of the sol-gel method described by Schertel et al. (2019)<sup>20</sup> to synthesize monodisperse amorphous titania colloids with a desired diameter of around 300 nm. The mechanics behind this reaction are further described in section 3.1 **Titania colloid synthesis by sol-gel method.** These titania colloids will then be forced to self-assemble into colloidal supraparticles, a term used for a cluster of colloids<sup>21</sup>.

There are different methods to trigger self-assembly to supraparticles. The driving force behind spontaneous self-assembly of the colloids is the difference in Gibbs free energy between the assembled state and the unassembled state of the system<sup>22</sup>. When the difference in free energy is negative it means that the energy decreases by inter-particle attractions in the self-assembled state, and is therefore the preferred state of the system. Typical forces between colloids are electrostatic, van der Waals or capillary forces. In this project we induced self-assembly mainly through the increase of the concentration and therefore the osmotic pressure of the colloids over time. This can be easily achieved through the drying of emulsion droplets. This two-step method requires to first synthesize the colloidal building blocks which are then dispersed in slowly drying emulsion droplets. This method of spherical confinement ensures symmetric self-assembly and can be applied to a wide range of particle mixtures or particles with a more complex shape<sup>23</sup>. Since only natural forces in a bottom-up fashion are applied with this approach, the method is very appealing for future bulk fabrication.

The advantage of supraparticles is that beside the properties of the individual colloids, new collective properties arise due to the near field coupling effects<sup>23</sup>, colocalization and structure of the colloids<sup>24</sup>. Of particular interest are supraparticles that exhibit optical, magnetic and catalytic properties. These new properties largely depend on the inherent properties, superstructure geometries and interparticle interactions of the colloids. In the case of monodisperse colloids, the supraparticles can self-assemble to photonic crystals, which are of major interest for applications in nanophotonics<sup>25</sup>. Overall, supraparticles could be a major player in new sustainable solutions. Depending on their properties they could be used in new more durable materials<sup>26</sup>, for cleaning up air pollution<sup>27</sup>, as sensors<sup>28</sup>, and even as tags for identifying and recycling materials<sup>29</sup>.

Supraparticles have already been formed with many different colloids, such as silica nanoparticles<sup>4</sup> and cobalt iron oxide nanoparticles<sup>30</sup>. Never before have above micrometre-sized crystalline supraparticles been synthesized with titania colloids. We expect that the optical properties of the supraparticles will be significantly improved by using titania colloids. When structured properly, the supraparticles will behave as photonic crystals in the visible light spectrum with emerging properties like Bragg reflection, light scattering and grating effects<sup>24</sup> and could be used in many optical applications including structural colouring, sensors and reflective displays<sup>4</sup>.

### 3 Theoretical background

In this section the synthesis methods and theory behind the experiments will be explained in more detail. The first section is about the theory behind titania colloid synthesis through a sol-gel method, followed by the mechanics behind silica coating and functionalisation of these titania colloids. The last section is about evaporation-induced self-assembly of the colloids, the technique used to form the supraparticles.

#### 3.1 Titania colloid synthesis by sol-gel method

Monodisperse amorphous titania colloids were synthesized using a sol-gel method described by Schertel et al. (2019)<sup>20</sup>, who adjusted the method from Tanaka et al. (2009)<sup>31</sup>. The main advantage of using this method is that it is easy to perform, a disadvantage is that it is difficult to control the speed of the reaction after it starts.

The exact mechanism of nanoparticle formation is not entirely clear, but LaMer's model<sup>32</sup> is a classical theory often used to describe the different stages of the reaction (figure 3.1)<sup>33</sup>. In stage I, the monomer concentration increases rapidly and reaches a threshold otherwise known as the critical nucleation concentration ( $C_{min}$ ). A monomer is a general term for a single molecule that is able to form long chains or 3D-networks with other monomers. When the monomer concentration surpasses the threshold, stage II starts and burst nucleation ensues. The quickly combining of the monomers into nuclei brings the concentration back below supersaturation. At this point stage III starts, which is the growth phase. The nuclei grow until an equilibrium is reached between monomer concentration and electrostatic repulsion charges between the particles. In this stage Ostwald Ripening<sup>34</sup> can also take place, where the matter of smaller and unstable particles divides over the other, larger, particles.

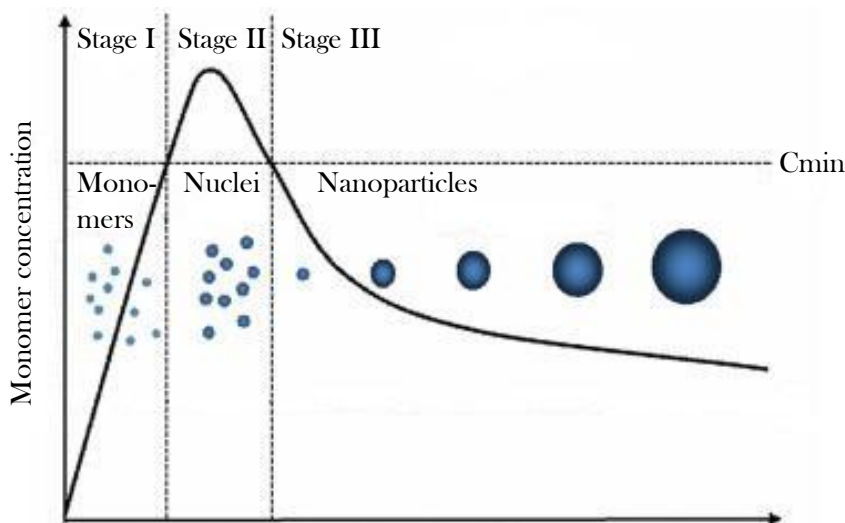


**Figure 3.1:** LaMer's model for nanoparticle formation. Adjusted from Mao et al. (2019).

A sol-gel synthesis typically consists of a non-aqueous liquid, a metal precursor, a catalyst and a hydrolysis agent<sup>35</sup>. In this solution oxygen-metal bonds will be formed through hydrolysis of the precursor followed by a polycondensation reaction which creates the 'gels' that will form the colloids.



In this work, titanium tetraisopropoxide (TTIP) is used as the metal precursor, dodecylamine (DDA) as catalyst, purified water as hydrolysis-agent and the solvent consists of a mixture of methanol and acetonitrile. In this reaction the DDA is also responsible for creating nanopores inside the titania colloids<sup>31</sup>. The first hydrolysis reaction of TTIP is visualised in figure 3.2 and can continue until the whole molecule is hydrolysed. The titanium hydroxide compounds, or monomers, are then able to form oxygen-metal bonds with other titanium hydroxide compounds or TTIP<sup>36</sup> (figure 3.3 and 3.4).

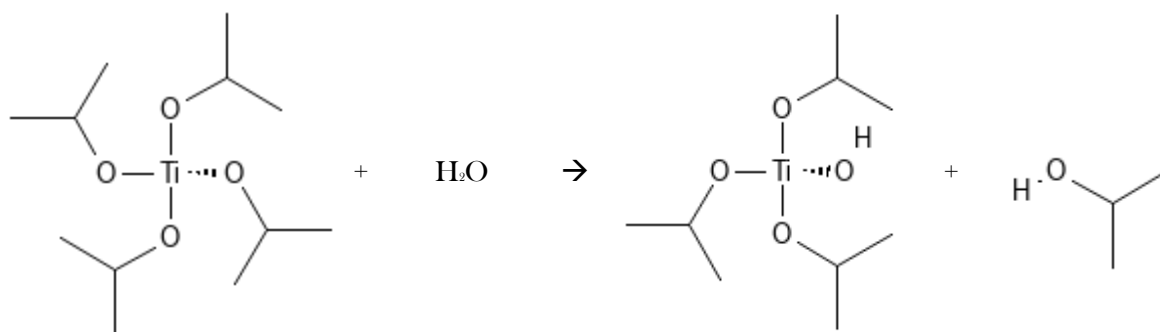


**Figure 3.2:** Single hydrolysis reaction of the titanium tetraisopropoxide (TTIP) precursor.

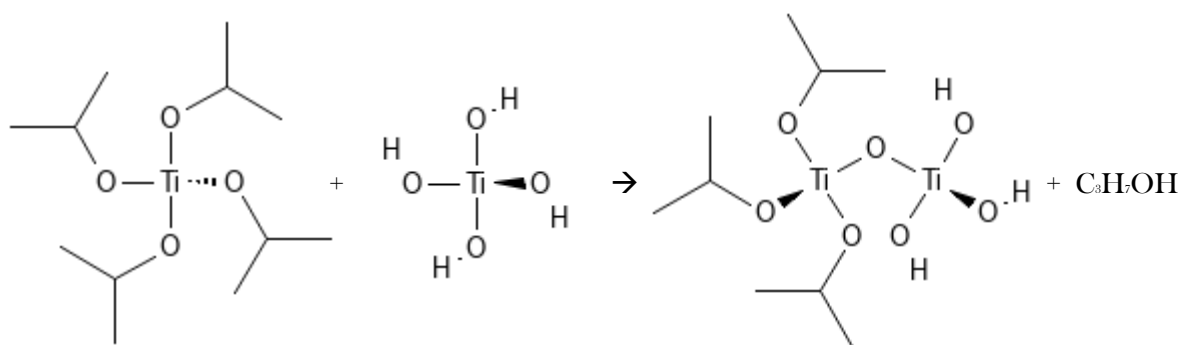


**Figure 3.3:** Alcohol elimination reaction of titanium tetraisopropoxide (TTIP) precursor and titanium hydroxide.

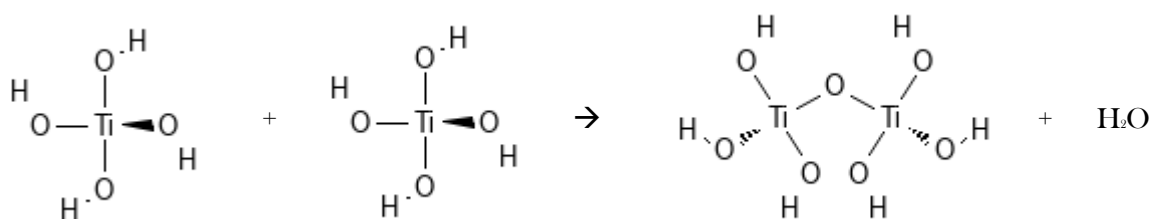


**Figure 3.4:** Condensation reaction of two titanium hydroxide compounds.

These reactions form small nuclei of titania hydrates with low electrostatic charges and high surface tensions. Hydrogen bonding and van der Waals forces then cause these small titania hydrates to agglomerate into larger networks until a certain electrostatic charge is reached. At this point the formed complexes will start to repulse and further growth is halted, signalling the end of the reaction<sup>6</sup>. At this point the colloids are formed.

A common issue in this type of reaction is the occurrence of a second nucleation phase. This can be prevented by only adding a small amount of hydrolysis agent or precursor such that nucleation can only happen once. However the amount of hydrolysis agent also determines the speed of the reaction and a

faster nucleation phase results in more nuclei and smaller colloids<sup>9</sup>. To synthesize monodisperse colloids of controllable size, an optimum concentration of the compounds is used.

### 3.2 Stöber method

Ever since the study by Stöber, Fink and Bohn in 1968<sup>37</sup>, the Stöber method has been the default for the synthesis of spherical silica colloids of controllable size<sup>38</sup>. The Stöber method is also based on sol-gel chemistry and uses the hydrolysis of a silicon alkoxide (figure 3.5), in this study tetraethyl orthosilicate (TEOS), as precursor and ammonia as catalyst. The colloids are formed from the condensation of the resulting silanol monomers. Ethanol is used as solvent and dissolves the apolar TEOS.

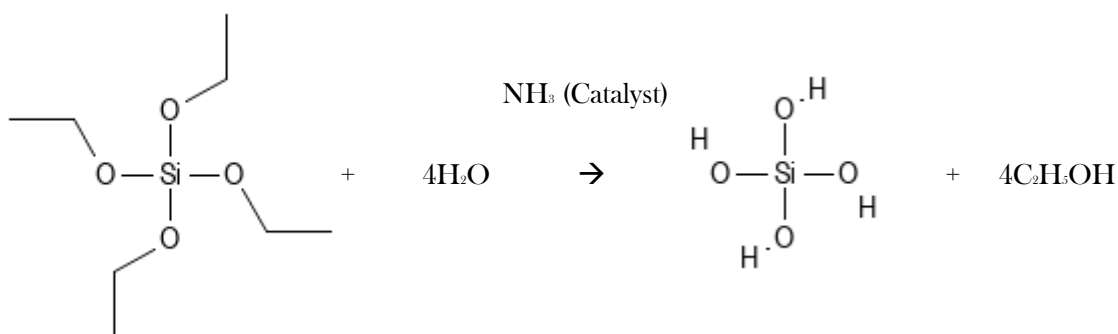


**Figure 3.5:** Hydrolysis reaction of tetraethyl orthosilicate (TEOS), producing silanol and ethanol.

In this work, the Stöber method is used to grow a silica layer around the titania colloids. Leftover hydroxyl groups on the surface of the titania colloids are able to bind with the silanol monomers, and subsequently the bound silanol monomers can bind with other silanol monomers. This network will eventually form a layer around the titania colloids and decrease polydispersity<sup>39</sup>. Other benefits of the silica layer are that it helps to stabilize the titania colloids by also binding within the pores of the colloids and that it facilitates functionalisation of the colloids. The silica surface can be modified with a coupling agent such that for instance the colloids can be doped with fluorophores or dispersed in nonpolar solvents.

### 3.3 Functionalisation

The silica coated titania colloids can be functionalised in different ways. For example, with fluorescent dye to make the silica layer visible with confocal microscopy. By using a coupling agent like (3-aminopropyl) triethoxy silane (APS), it was possible to dye the colloids with fluorescein isothiocyanate (FITC)<sup>40,41</sup> (figure 3.6). APS reacts in a similar way as TEOS and can create a network through hydrolysis and condensation reactions in a Stöber mixture.

The colloids in this work were also functionalised with octadecyltrimethoxysilane (OTMOS)<sup>42</sup>, which is a coupling agent and has a functional group attached (figure 3.7). The methoxy groups of OTMOS are very reactive and can bind to free hydroxyl groups in the silanol network. The C<sub>18</sub> tail of the OTMOS makes it possible to disperse the colloids in nonpolar solvents such as oil, this is necessary for the supraparticle experiments where we use oil emulsion droplets.

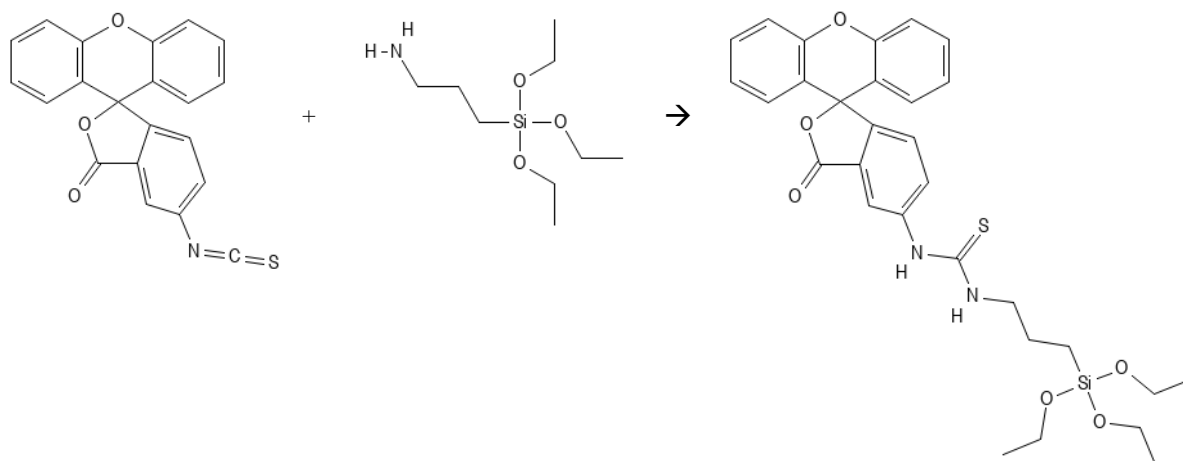


**Figure 3.6:** Binding of fluorescein isothiocyanate (FITC) to the coupling agent (3-aminopropyl) triethoxy silane (APS)

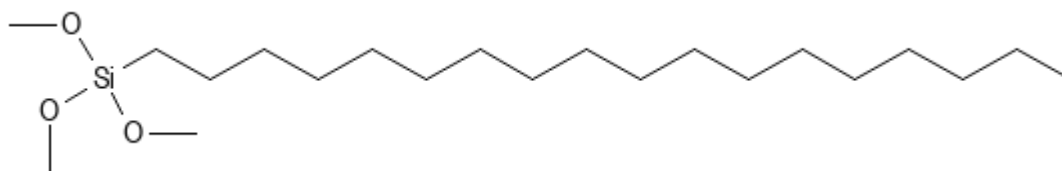


**Figure 3.7:** Octadecyltrimethoxysilane (OTMOS) molecule

### 3.4 Self-assembly through spherical confinement

The synthesized titania-silica colloids are forced to self-assemble inside a spherical confinement by slow evaporation of the solvent. The resulting cluster of colloids is called a ‘supraparticle’, a term first used by Velev et al. (1996)<sup>21</sup>. The method of spherical confinement has both been tested in experimental and computational set-ups, and proven to work by both<sup>30,42-45</sup>.

The mechanics are simple, the system consists of a polar and nonpolar droplet-emulsion stabilized by a surfactant. The colloids are dispersed in the discontinuous phase which has a lower boiling point than the continuous phase. The difference in boiling point allows the emulsion droplets to evaporate faster than the continuous phase, causing them to shrink. The more the emulsion droplets shrink, the more the colloids are forced to interact. This entropy driven-process causes the colloids to self-assemble in their lowest free energy state (figure 3.8). Only if the evaporation is slow enough will the colloids be able to reach this lowest free energy state, which is found to be icosahedral (five-fold) symmetrical clustering for systems up to 100 000 particles with hard interactions and thus entropy alone<sup>30</sup>. A too high polydispersity can also hinder the ordering and therefore the aim is to use monodisperse colloids with a polydispersity below 5%<sup>46</sup>.

If evaporation goes too fast, the formation of ‘onion-shaped’ supraparticles generally takes place<sup>4</sup>. Onion-shaped supraparticles, also called ‘supraballs’, are colloidal crystals consisting of radially layered face-centered-cubic (FCC) colloids (figure 3.9A). However the formation of defects in onion-shaped supraparticles is unavoidable since this type of packing of the colloids does not equal a perfectly spherical surface<sup>47</sup>. Furthermore, deeper within the onion-shaped supraparticle the colloids could be in disarray because of the high curvature inside. These distortions can cause random scattering and incoherent Bragg diffraction, which suppresses structural resonance and subsequently lowers the optical performance of the supraball<sup>5</sup>.

However, as proposed by Charles Frank in 1952<sup>48</sup>, it was shown that the entropically favourable structure actually was the one of an icosahedral crystal<sup>30</sup>. An icosahedral cluster consists of 20 grains of tetrahedral wedges with deformed FCC crystals, has five-fold symmetry and is formed around a central particle surrounded by twelve other particles<sup>3</sup>. When these crystals grow further they become rhombicosidodecahedron-shaped (figure 3.9B), but maintain the icosahedral core. This fully ordered structure does not have any distortions in the arrays of the colloids which reduces incoherent light scattering and significantly improves the optical properties of the supraparticles. Making them more preferable for optical applications<sup>4</sup>. The first research to manage to create these icosahedral supraparticles was from Bart de Nijs and co-workers<sup>30</sup>. Proving that the hard interparticle interactions combined with Evaporation Induced Self-Assembly (EISA) is actually sufficient for creating these icosahedral supraparticles. Provided that the number of particles inside the droplets is not too high, the interactions are hard=sphere like and evaporation of the emulsion droplets slow enough to reach the equilibrium lowest free-energy state.

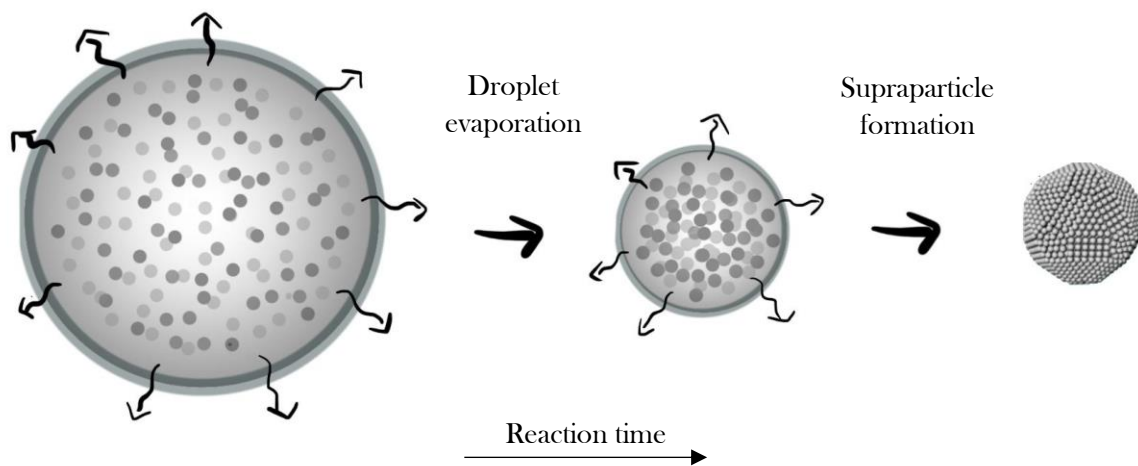


**Figure 3.8:** Evaporation-induced self-assembly of colloids.

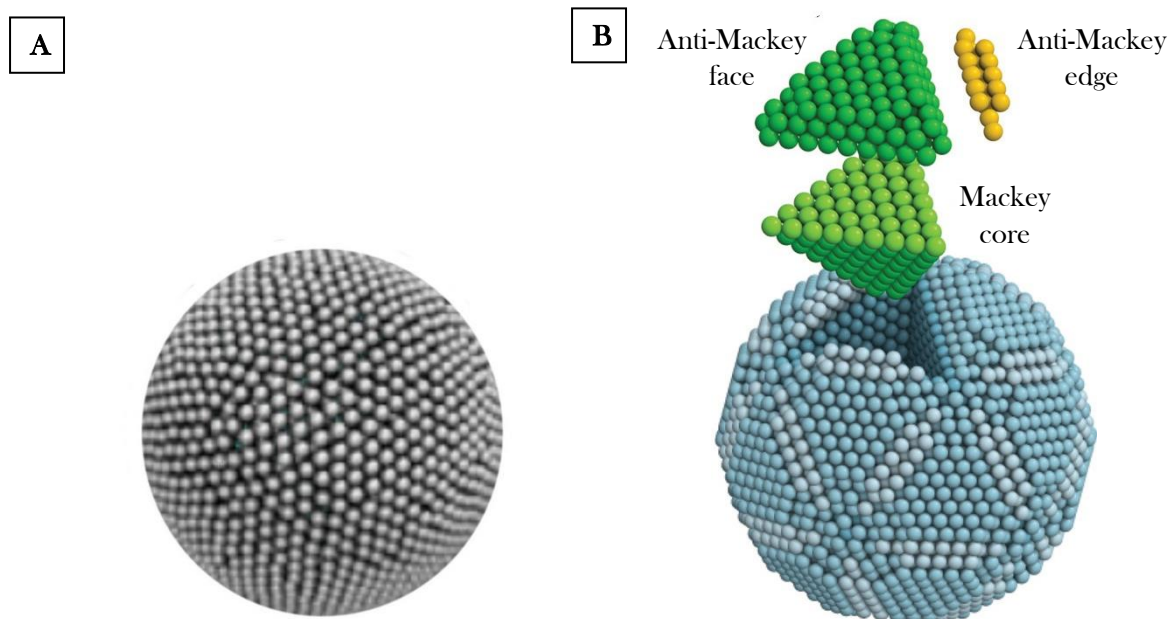


**Figure 3.9:** (a) Onion-shaped supraparticle consisting of radially layered FCC colloids. (b) Icosahedral supraparticle consisting of 20 grains of tetrahedral wedges. Adjusted from Wang et al. (2020).

## 4 Results and discussion

### 4.1 Titania colloid synthesis

Monodisperse titania colloids with a diameter of 438 nm and a polydispersity of 6% were synthesized with a sol-gel method described by Schertel et al. (2019)<sup>20</sup> and characterised with Transmission Electron Microscopy (TEM) (figure 4.1 A & B). The monodispersity of the sample was also discernible by eye since holding the sample to the light showed iridescent colours after concentrating the particle enough, which only occurs when the colloids are of similar size (figure 4.1C).

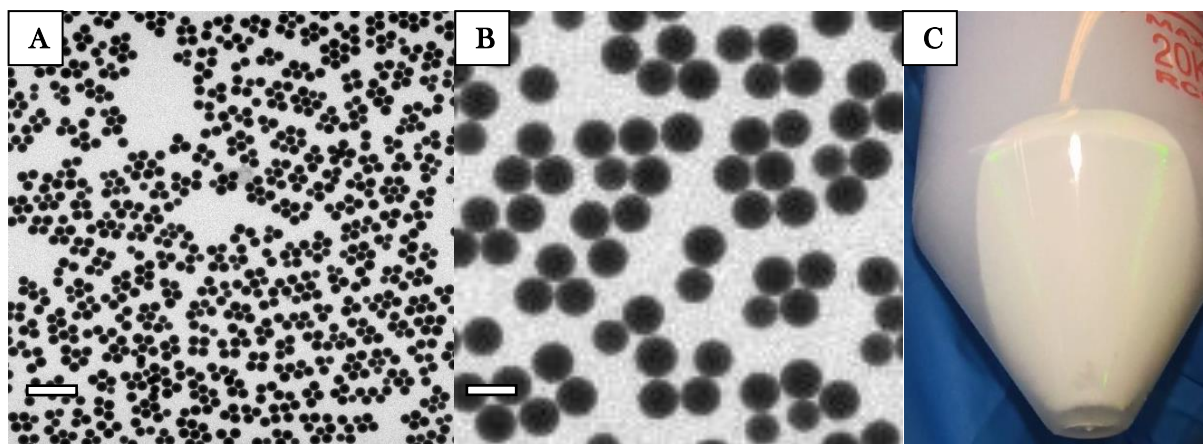


**Figure 4.1:** (a & b) TEM images of monodisperse titania colloids. Diameter  $438 \pm 26.72$  (6%) nm (Scale bar: 2  $\mu\text{m}$  and 500 nm respectively). (c) Iridescence of the sedimented titania colloids as visible by eye in the lab.

These colloids were primarily used in the further silica coating and supraparticle experiments.

#### 4.1.1 Titania size experiments

Since colloids with a diameter of 300 nm require less time to self-assemble<sup>25</sup> and interfere differently with light in the visible spectrum, a few experiments were conducted with the aim to decrease the size of the titania colloids. Schertel et al. (2019) showed that varying the amount of water and DDA in the synthesis results in different sizes, but also a difference in monodispersity. An experiment where 900  $\mu\text{L}$  water was added instead of 700  $\mu\text{L}$  resulted in smaller, but more polydisperse colloids (figure 4.2A). The same result was observed when the amount of water was increased to 1200  $\mu\text{L}$  but the molar ratio with DDA was kept the same by adding 1.71 grams of DDA instead of 1 gram (figure 4.2B). In a final experiment there were no alterations made to the experimental parameters but the colloids were analysed after 2 hours (h), 4 h, 6 h and 8 h of synthesis. We observed smaller titania colloids in the 4 hour sample, however these colloids were a lot more porous and less stable than those of the 8 h sample (figure 4.2C). It is unknown why the colloids did not grow uniformly over time.

#### 4.1.2 Condensation experiments

The titania colloids were not very stable in solvents beside methanol (Appendix figure 1). We suspected that this was partly due to the pores inside the titania colloids, making them easier to dissolve in the ethanol and subsequently decrease in size and uniformity. Therefore, to make the titania colloids more stable, we tried to condense the colloids in a few heating experiments. The titania colloids were heated in 80  $^{\circ}\text{C}$  water with 0.74 M ammonia for 65 h and in another experiment in 40  $^{\circ}\text{C}$  methanol for 19 h. Both experiments did not show the desired results. After heating the titania colloids in water, the pore size increased, likely due to dissolution of the titania (figure 4.3A). After heating in methanol, the colloids decreased in size but ‘clouds’ in the TEM sample let us suspect that this is not due to condensation but dissolution and the falling apart of the titania colloids (figure 4.3B). Both samples lost the desired

iridescent property of monodisperse titania colloids. In another experiment the colloids were dried and heated under a heat lamp, but this resulted in deformations of the colloids. The colloids were unable to

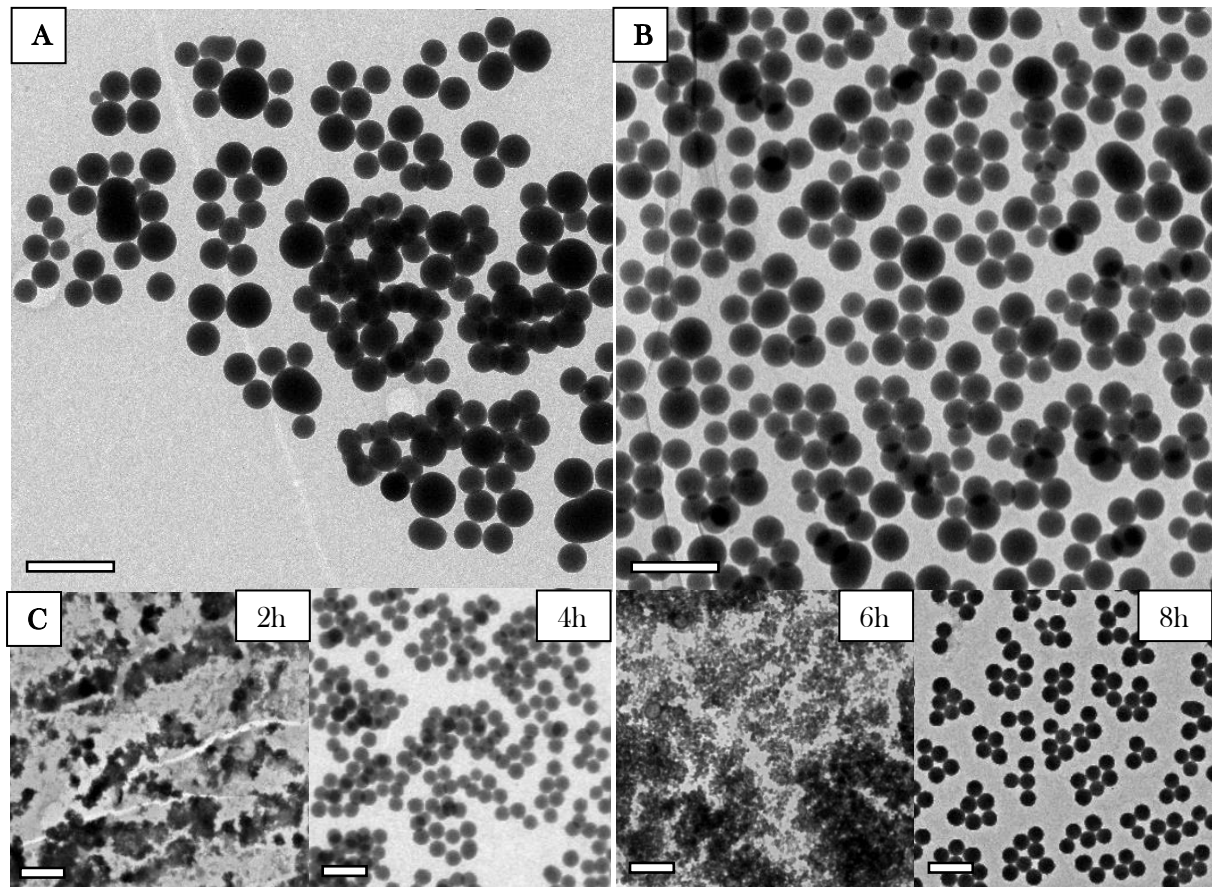


**Figure 4.2:** TEM images of titania colloids. (a) Experiment with 900  $\mu\text{L}$  water, average diameter of  $378\pm 68$  (18%) nm (scale bar: 1  $\mu\text{m}$ ) (b) Experiment with higher DDA/water ratio, average diameter of  $360\pm 60$  (17%) nm (scale bar: 1  $\mu\text{m}$ ). (c) Samples from different timepoints during titania colloid synthesis (scale bar: 1  $\mu\text{m}$ ). The 2 h sample shows no colloids, the 4 h sample shows very porous colloids (diameter of  $355\pm 29$  nm), the 6 h sample only shows secondary nucleation and the 8 h sample shows the expected titania colloids (diameter of  $420\pm 22$  nm).

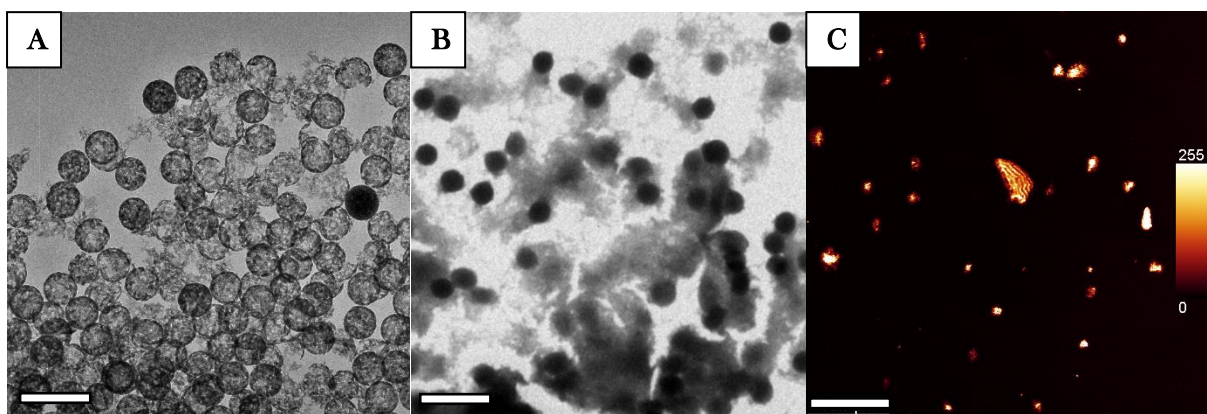


**Figure 4.3:** Images of titania colloids after condensation experiments. (a) TEM image of titania colloids after heating for 65 h in 80  $^{\circ}\text{C}$  water with 0.74 M ammonia (scale bar: 1  $\mu\text{m}$ ). (b) TEM image of titania colloids after heating for 19 h in 50  $^{\circ}\text{C}$  methanol (scale bar: 1  $\mu\text{m}$ ). (c) Confocal image of large chunks of titania after heating titania colloids under the heat lamp (scale bar: 16  $\mu\text{m}$ ).

fully redisperse in methanol and large chunks of titania were aggregated (figure 4.3C).

## 4.2 Stöber silica coating

To stabilize the titania colloids in different solvents and to facilitate functionalizing them, a silica layer was added to the colloids using the Stöber method in combination with seeded growth<sup>39</sup>. The aim was to create titania-silica core-shell colloids with a layer thickness of around 50 nm.

### 4.2.1 FITC functionalisation

In a first set of experiments fluorescein isothiocyanate (FITC) after it had chemically formed a bond with a so-called silane coupling agent<sup>40</sup>, was added to the silica layer. A thin second silica layer was added to encapsulate the first layer with FITC. The FITC made it possible to image the first silica layer separately from the titania colloid with confocal microscopy and also facilitated imaging the individual colloids since the high refractive index of the titania colloids causes a lot of light scattering in the reflective signal. Figure 4.4 shows a confocal image of successfully synthesized titania-silica colloids in ethanol where a fluorescent signal surrounding the colloids can be seen. However, the highest fluorescent signal comes from the middle of the colloids. This could be because of the accumulation of the fluorescent signal in the z-direction or/and that the dye is also present in the titania colloids itself. In a different experiment, Energy Dispersive X-Ray (EDX) images showed that silica was also present within the titania colloids, filling up the pores (figure 4.7). It is therefore likely that the FITC dye was indeed also present within the titania colloids, explaining the bright fluorescent signal at the centre of the confocal images.

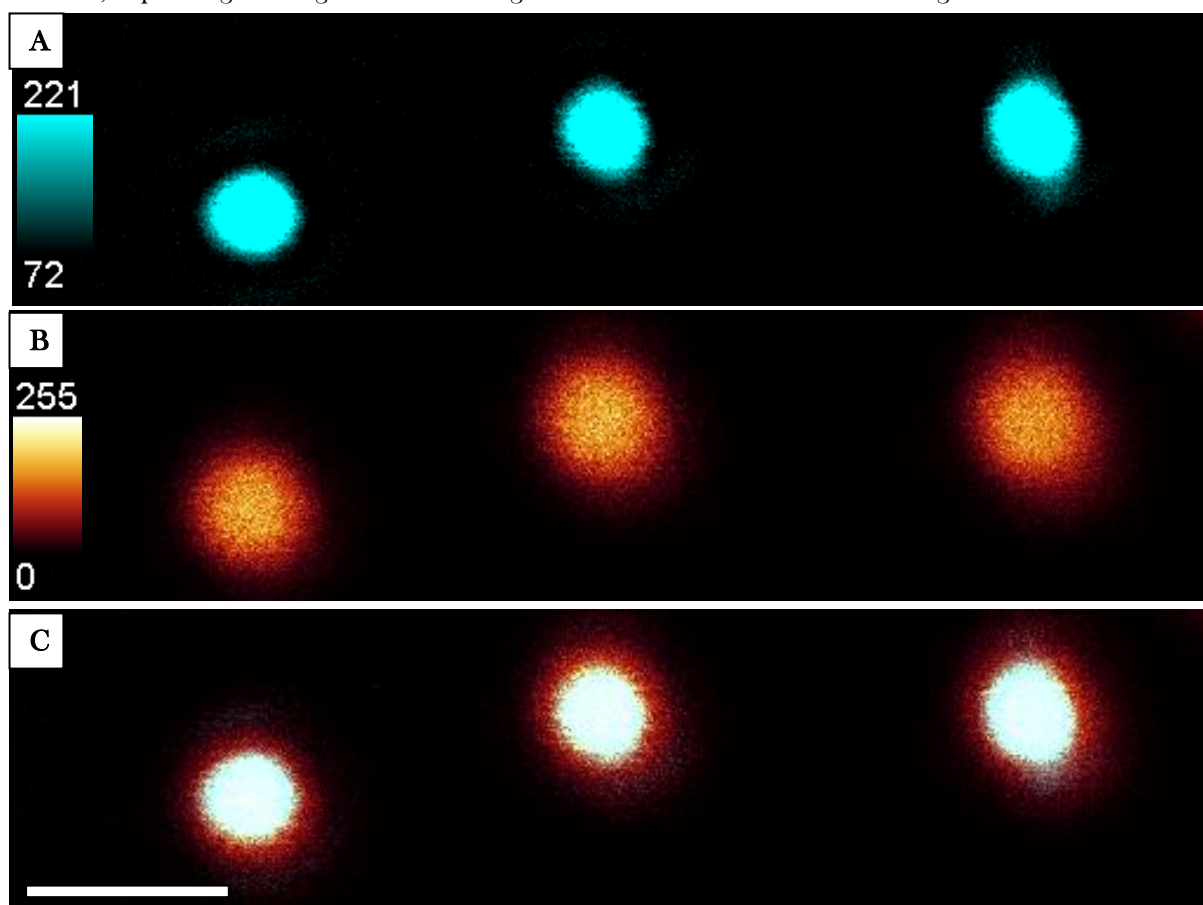


**Figure 4.4:** Leica SP8 confocal images of titania-silica colloids in ethanol (scale bar 1  $\mu\text{m}$ ). (a) Reflective signal of the titania colloids. (b) Fluorescent signal of the FITC-silica layer. (c) Merged channels.

Unfortunately, TEM and confocal images showed many aggregated FITC colloids (figure 4.5). It is unclear why this happened, but since titania colloids with a single silica layer did not appear to have the same problem, it could either be caused by the addition of a second silica layer or the coupling agent (3-aminopropyl) triethoxy silane (APS). Aggregated colloids are detrimental for crystalline supraparticle

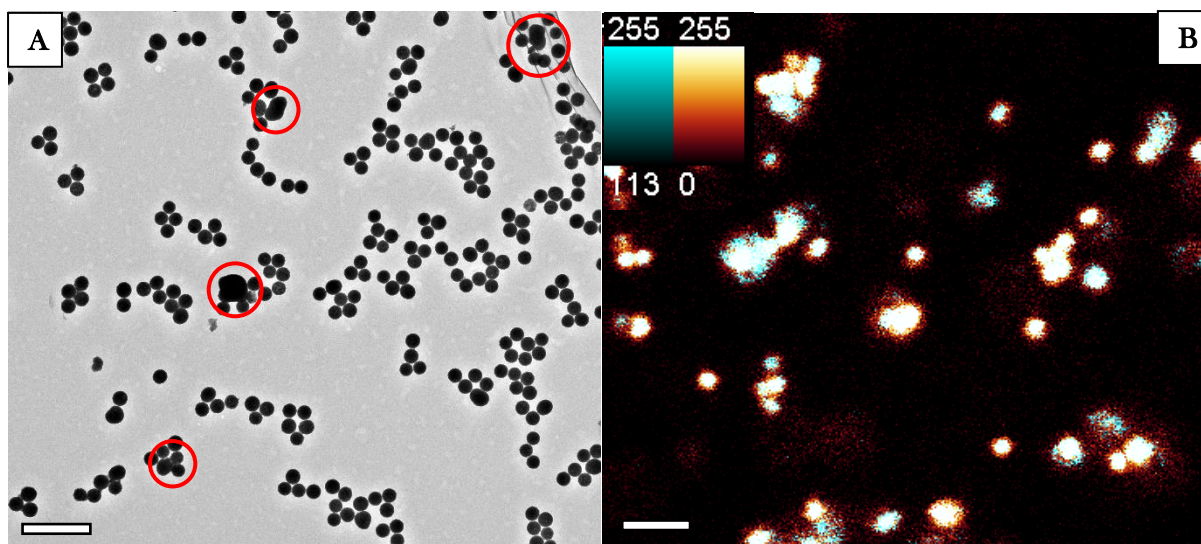


**Figure 4.5:** Titania colloids coated with a FITC-APS-Silica layer (Scale bar: 2  $\mu\text{m}$ ) (a) TEM image of the colloids with a few examples of aggregates and dumbbells. (b) Merged confocal image of the colloids showing multiple aggregates and dumbbells (still from a movie). Merged channels are the reflection signal in blue and fluorescent signal in orange.

formation. It is possible to separate the aggregated particles from the individual particles. However, this would require a lot of extra centrifugation steps and confocal analyses. In the end, it was decided to use titania colloids with a single silica layer and without FITC in further experiments because their synthesis was significantly less time-consuming and yielded better results overall.

#### 4.2.2 Single silica layer

Since an extra fluorescent layer increased the size of the colloids and seemed to cause aggregation in multiple samples, it was decided to omit the FITC in further experiments. The titania colloids (figure 4.1) were coated with a single silica layer and characterized with TEM images (figure 4.6 A & B) and confocal microscopy, which showed that the individual particles were freely diffusing. The polydispersity of the titania-silica colloids was 3%, perfectly adequate for use in the supraparticle experiments wherefore the aim was to use colloids with a polydispersity below 5%. Again, iridescence of the sample was visible by eye (figure 4.6C). The TEM images showed a slight decrease in diameter size of the colloids, which went against expectations. EDX images showed why this was the case (figure 4.7). Instead of a silica layer around the titania colloids, a titania-silica composite had formed. Most likely the silica invaded the pores of the titania colloids. The EDX spectrum-composition showed an almost perfectly even amount of silica and titania particles (Appendix 10.2). The slightly smaller diameter could be further explained by calibration errors of the TEM, dissolution of part of the titania in the ethanol or just a small measurement error in the polydispersity analysis.

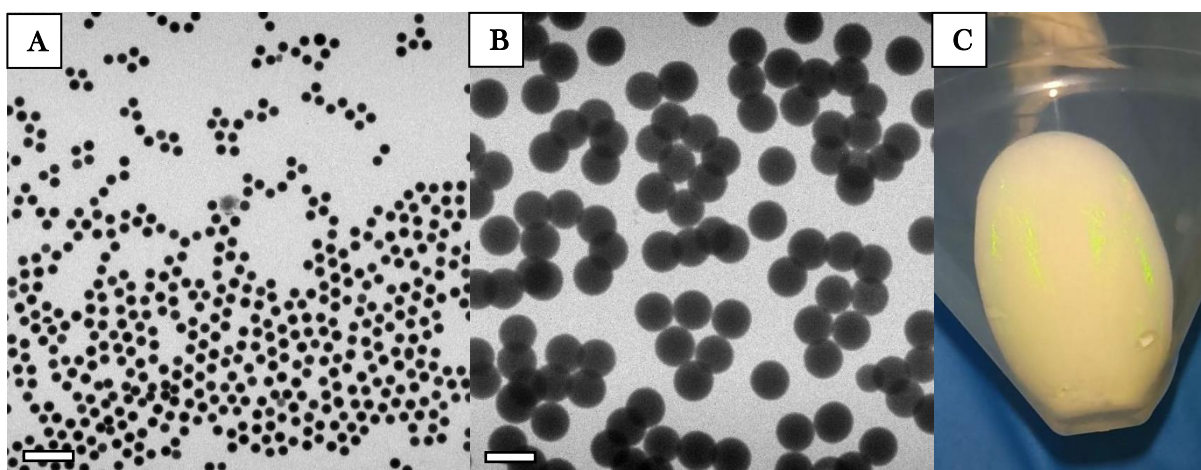


**Figure 4.6:** (a & b) TEM image of silica coated titania colloids with a diameter of  $421 \pm 14$  (3%) nm. (Scale bar: 2  $\mu\text{m}$  and 500 nm respectively) (c) Iridescence of the sedimented titania-silica colloids as visible by eye in the lab.



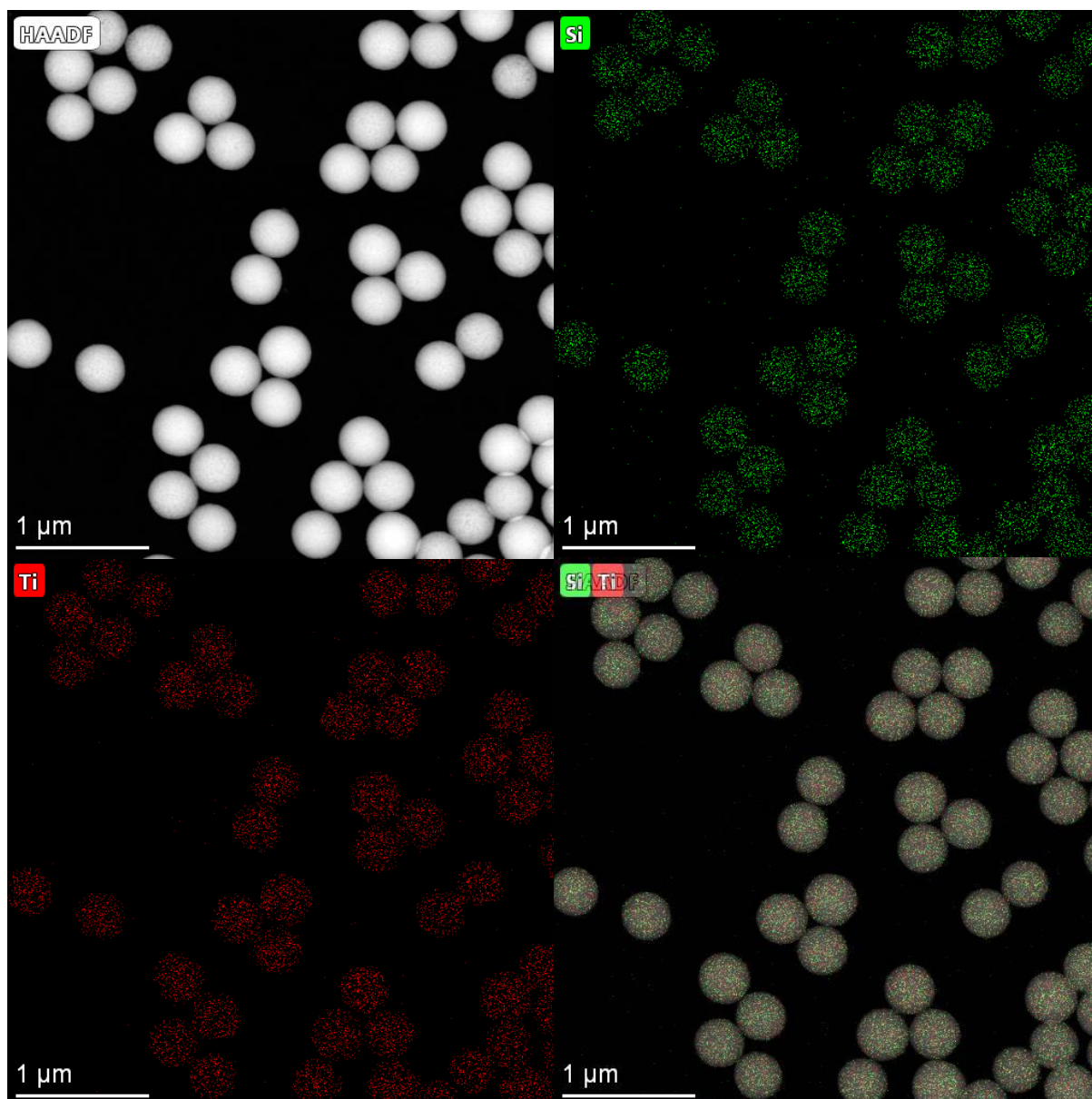


**Figure 4.7:** EDX images of the silica coated titania colloids. Merged image has a 65% transparent high-angle annular dark-field (HAADF) overlay.

### 4.3 OTMOS functionalisation

To be able to disperse the titania-silica composites in oil, an octadecyltrimethoxysilane (OTMOS) coating was added to the titania-silica composites (figure 4.8). Due to the C18-chain of OTMOS a maximum layer of 10 nm was expected around the titania-silica composites. However, a layer of around 42.6 nm was found. Figure 4.9 shows the EDX images of these colloids, which have a very similar composition to the titania-silica composites, only bigger. The reason for this seemingly swelling of the colloids is unclear, it could be that the OTMOS somehow interacts with the pores of the composites or that the prolonged sonication and subsequently heating of the colloids during the coating caused the swelling or the calibration of the TEM microscope could be slightly incorrect. These colloids did not show any iridescent behaviour even though they were monodisperse (4%). It could be that the added carbon in the C18-chains absorbs some of the scattering light<sup>4</sup> or the volume fraction of titania reached below 55%, in which case iridescence would not be seen. The OTMOS coating did seem to cause a few colloids to aggregate (figure 4.8) but since this was only a small percentage the particles were still used in the supraparticle experiments.

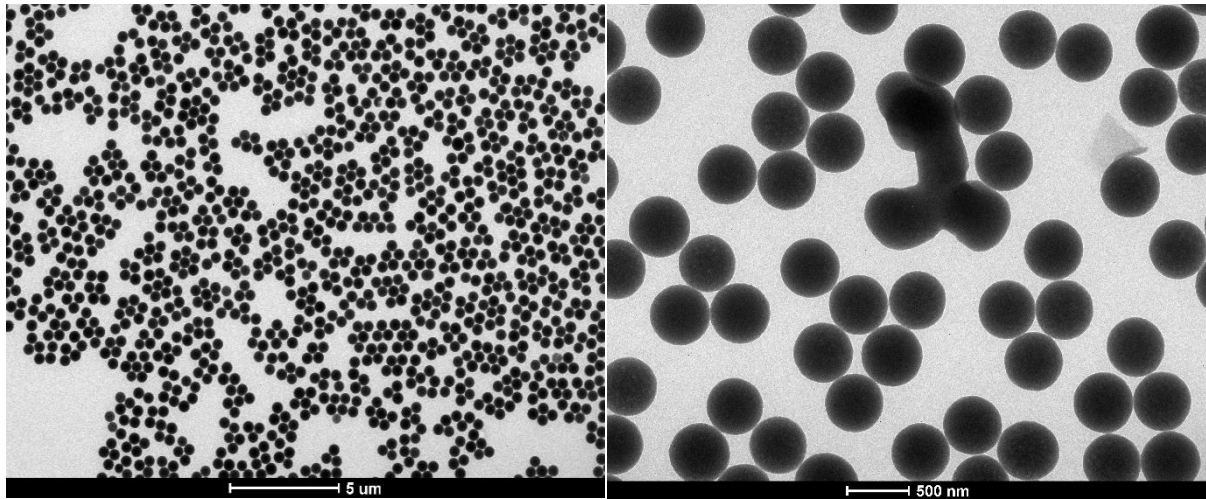


Figure 4.8: TEM images of OTMOS coated titania-silica composites with a diameter of  $506.4 \pm 20.18$  (4%) nm.

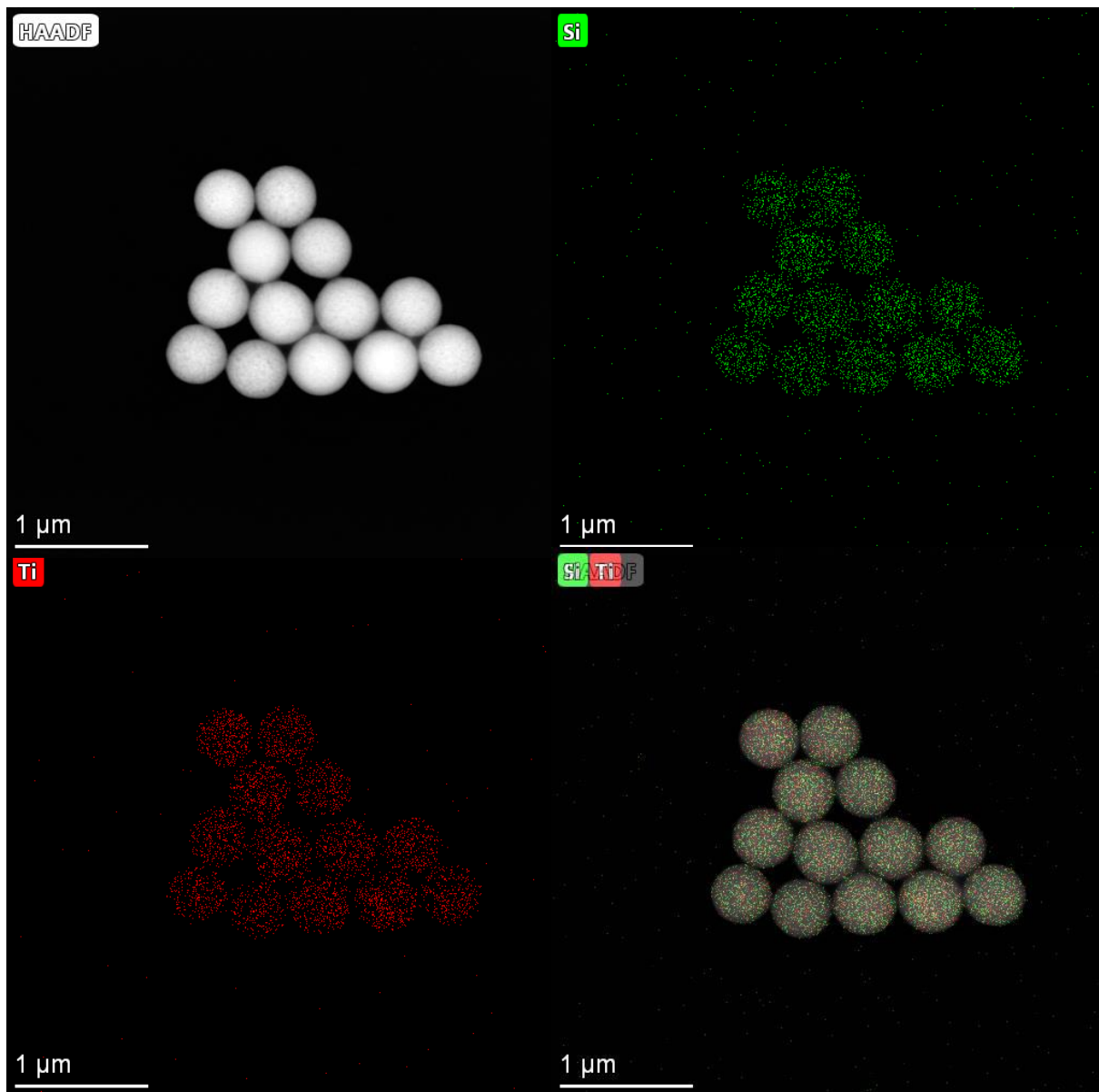
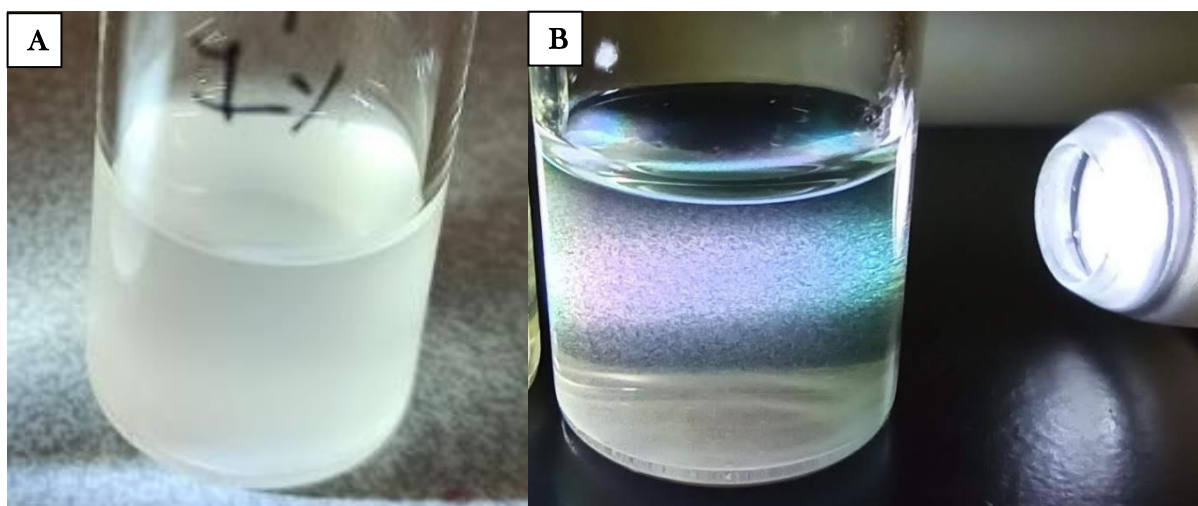


Figure 4.9: EDX imaged of the OTMOS coated titania-silica composites. Merged image has a 65% transparent HAADF overlay

## 4.4 Supraparticles

To synthesize our supraparticles, a technique called Evaporation Induced Self-Assembly (EISA) was used. Emulsion droplets were formed by vigorously shaking of a sample containing dispersed colloids into a discontinuous phase and a continuous phase with an opposite polarity and higher boiling point. This method generates very polydisperse emulsion droplets meaning that supraparticles of different sizes will be formed. Slow drying of the emulsion droplets enforced the self-assembly of the colloids into supraparticles. Onion-shaped and icosahedral shaped supraparticles are formed after, respectively, fast and slow evaporation of the discontinuous phase.<sup>4</sup> Due to the polydispersity of the emulsion droplets, some droplets dried sooner than others. To try to determine whether the supraparticles were formed, a broad spectrum penlight was shined through the sample. When iridescent colours were observed it meant that ordered structures were present in the sample (figure 4.10B), however because of the polydispersity of the emulsion droplets this did not necessarily mean that all emulsion droplets had evaporated. If only white or scattering light was observed when shining through the sample, it meant that the colloids were not yet structured and that the emulsion droplets were still present (figure 4.10A).



**Figure 4.10:** Water in oil supraparticle synthesis, samples are illuminated with a broad spectrum pen light. Pictures taken with a Xiaomi Redmi Note 8 pro mobile phone. (a) Water emulsion droplets with dispersed titania-silica composites in hexadecane. (b) Iridescence of supraparticles after emulsion droplet evaporation and washing with hexane. The supraparticles are blurred in this image because they are moving.

### 4.4.1 Water in oil

The titania-silica composites (figure 4.6) were dispersed in water and emulsified in water saturated hexadecane. It was necessary to saturate the hexadecane with water since it suppressed the outflux of water from the emulsion droplet, thereby reducing the rate of droplet evaporation. Too fast evaporation of the emulsion droplets resulted in amorphous supraparticles (figure 4.11B). It was found that a single layer of parafilm, too high colloid v/v%, multiple evaporation holes, additional manual shaking of the sample during incubation on the shaker and anhydrous hexadecane all resulted in these amorphous supraparticles. Another critical parameter was the incubation time. When the supraparticles were washed too soon (<7 days), like at the first signs of iridescent colours emerging, the supraparticles collapsed during the washing steps or Scanning Electron Microscopy (SEM) imaging (figure 4.11A). The supraparticles seemed to aggregate (figure 4.11C) when the sample was not entirely clean or the diameter of the glass vial too small (4 mL vial). Debris in the sample, caused by an uncleaned septum stopper, probably interfered with the emulsion droplets, allowing them to aggregate which subsequently led to aggregated supraparticles. A vial with a too small diameter could cause the emulsion droplets to stack on top of each other when they sediment, thereby causing supraparticles to aggregate after drying of the emulsion droplets. Eventually, different supraparticles crystalline structures and sizes were achieved by varying the v/v% of the colloids inside the emulsion droplets and the glass vial size.

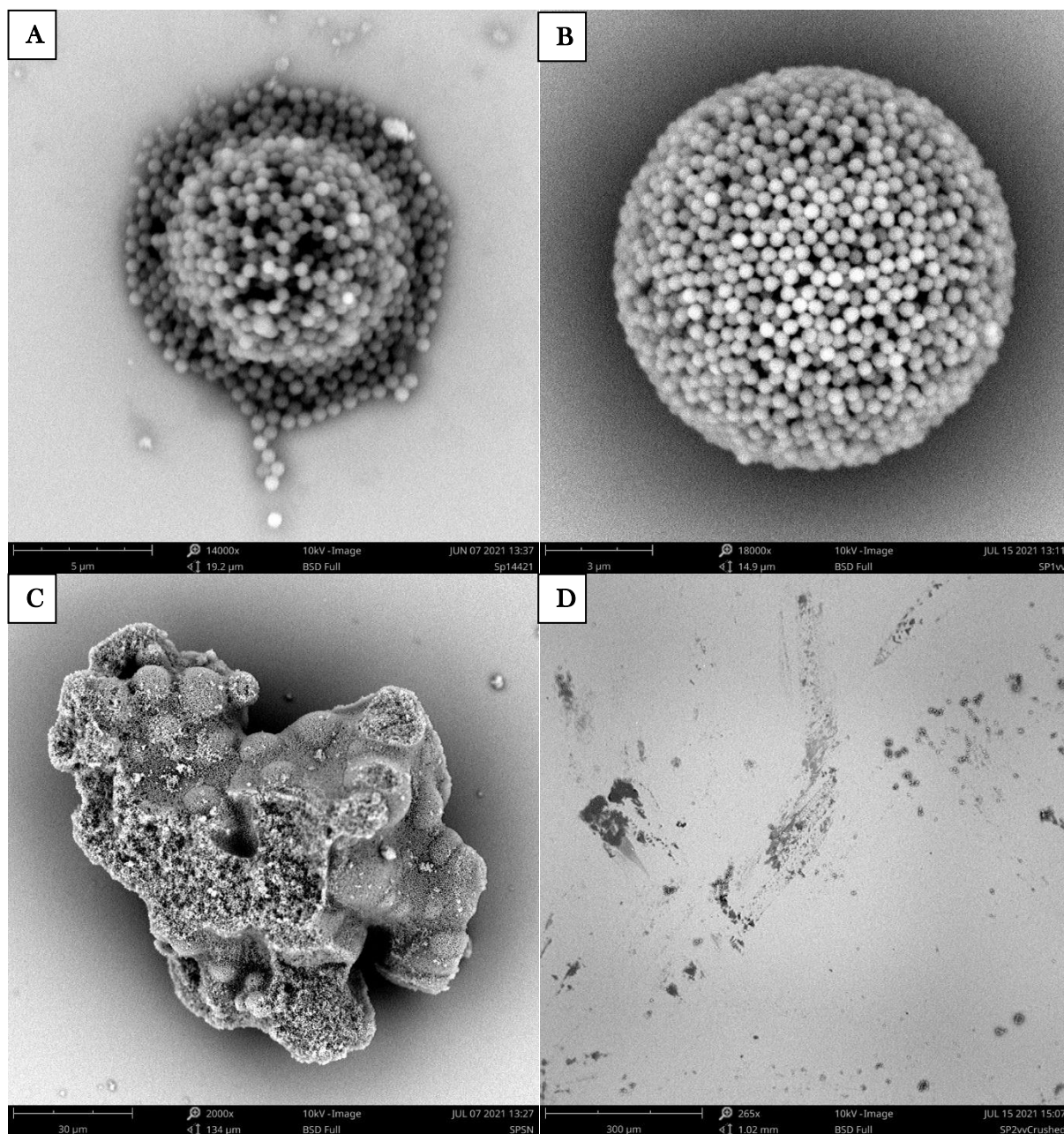


**Figure 4.11:** Reasons why some of the water in oil supraparticle formation experiments failed. (a) Washing before sample is completely dry, the supraparticles are unstable and collapse. (b) Evaporation is too fast, amorphous colloidal supraparticles are formed. (c) Sample is a bit dirty and evaporation way too fast or the vial is too small, a lot of aggregates are formed. (d) Trying to image broken supraparticles by scratching the sample, was not successful.

The most uniform onion-shaped supraparticles were formed with a 3 v/v % titania-silica composites and a 20 mL glass vial after drying for 26 days (figure 4.12). However, a different sample proved that washing after 7 days of drying was also sufficient. Broken supraparticles in the sample showed that the supraparticles were not hollow and had highly structured outside layers (figure 4.12D). Only broken particles already present in the sample were imaged since manually breaking of the particles by trying to scratch the SEM sample surface did not result in clean cuts of the supraparticles (figure 4.11D). The inside structure of the onion-shaped supraparticles was also visible in slices of confocal Z-stacks of the supraparticles (figure 4.13A&B), especially compared to the confocal images of amorphous supraparticles (figure 4.13C). It looks like the supraparticles with a diameter of 8 μm had around 4 structured outside colloid layers and an unstructured centre and that bigger supraparticles had the same sized unstructured core only more structured outside layers, as can be seen in figure 4.13B were a supraparticle of 14 μm has around 8 structured outside colloid layers. That the cores are unstructured is not surprising, the high

curvature at the centre of the particle makes it impossible for the colloids to maintain the same crystalline structure<sup>4</sup>. Unfortunately, the light scattering caused by the colloids made it difficult to identify individual colloids, rendering an exact analysis of these confocal images almost impossible. However, a general trend and structure is certainly visible. The onion-shaped structure was observable in all supraparticle sizes ranging between 4 and 30  $\mu\text{m}$  (figure 4.12A) and they showed iridescent colours when illuminating with a broad spectrum pen light. Optical microscope images showed the behaviour of light when the particles were illuminated (figure 4.12B). The supraparticles seem to be largely of uniform colour, with some visible grating diffraction effects.

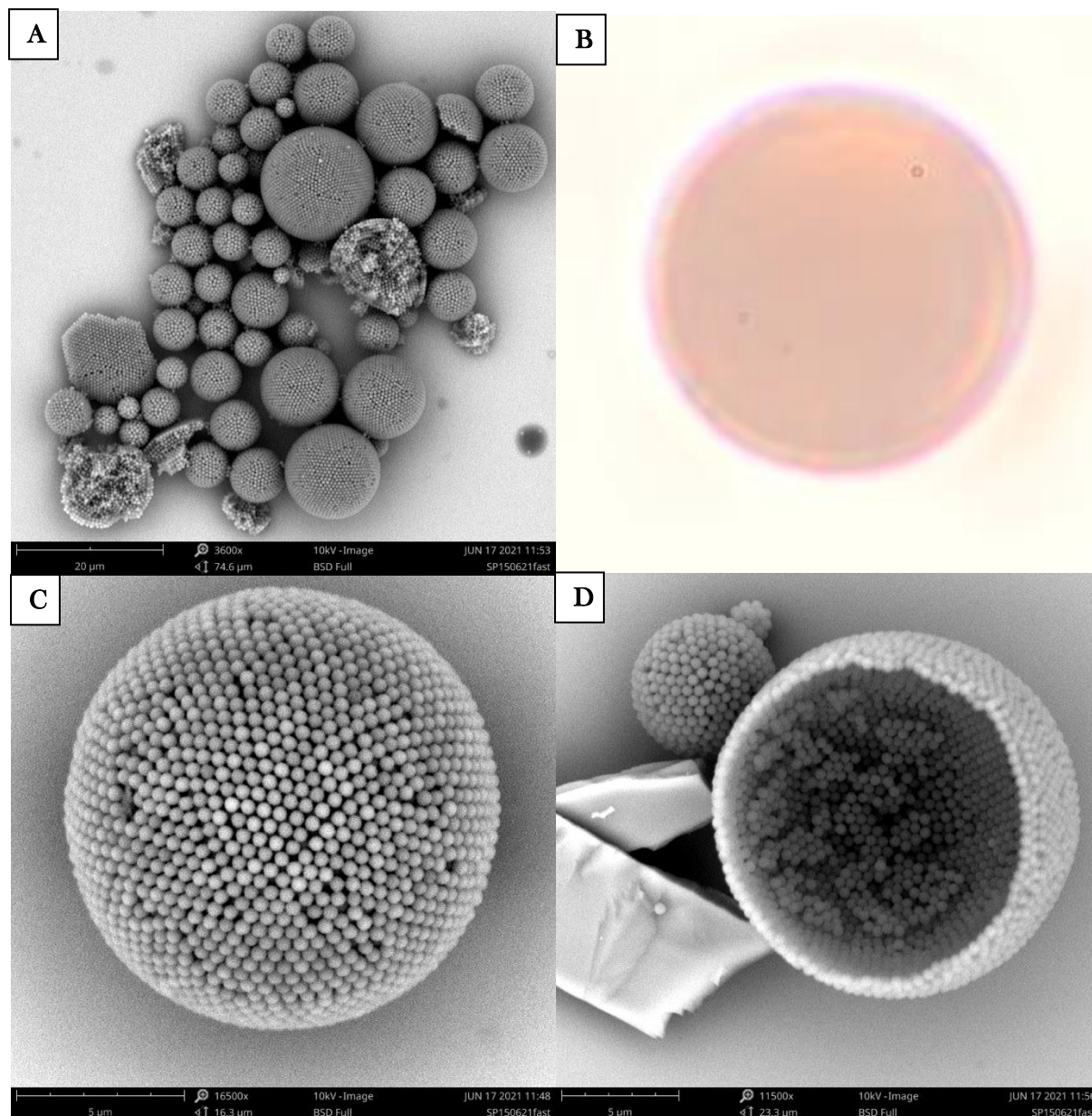


**Figure 4.12:** SEM images of onion-shaped supraparticles. (a) Overview of differently sized supraparticles with onion-shaped structure. (b) Optical microscope image of an onion-shaped supraparticle. (c) single onion-shaped supraparticle with a diameter of 13.2  $\mu\text{m}$ . (d) SEM image of a broken supraparticle with a diameter of 15.6  $\mu\text{m}$ , showing an ordered structure within the supraparticle.

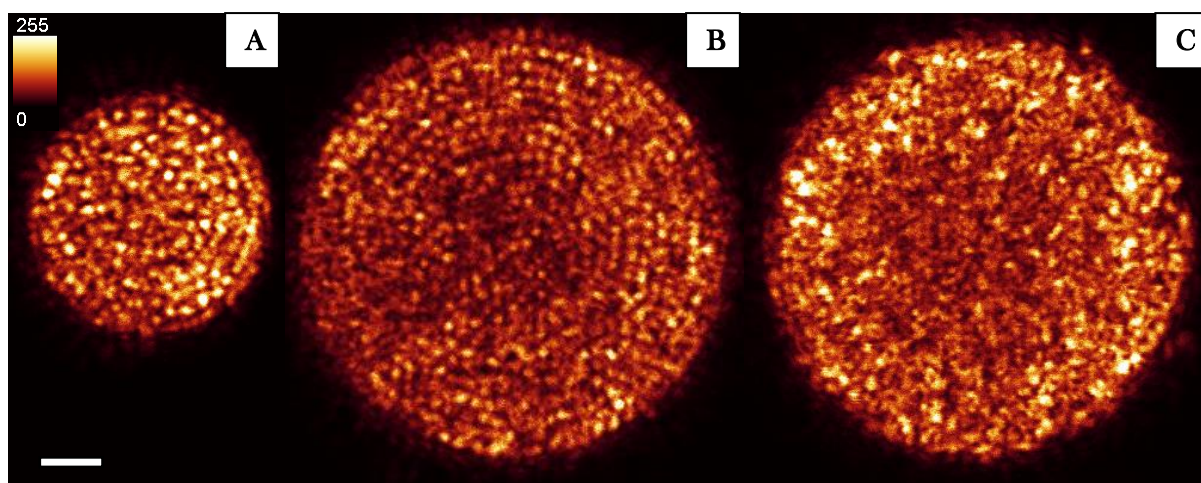


**Figure 4.13:** Inside slices of confocal Z-stacks of supraparticles, showing the reflection signal of the colloids. The supraparticles were dissolved in hexane. (Scale bar: 2  $\mu\text{m}$ ) (a) Onion-shaped supraparticle with a diameter of 8  $\mu\text{m}$ . (b) Onion-shaped supraparticle with a diameter of 14  $\mu\text{m}$ . (c) Amorphous supraparticle with a diameter of 13  $\mu\text{m}$ .

The best icosahedral supraparticles were formed with a 2-3 v/v% of titania-silica composites and a 7 mL glass vial (figure 4.14), however more than 50% of the supraparticles remained (partially) onion-shaped. A smaller glass vial resulted in more aggregated supraparticles and not more icosahedral structures, so slowing down the emulsion droplet evaporation with this method was not possible. Since the vial size and the number of evaporation holes could not be decreased further, the next step was to try to decrease the volume/volume fraction of the colloids inside the emulsion droplets. The expectation was that when the number of colloids per emulsion droplet decreased, but the size of the emulsion droplets remained the same, the colloids would have more time to self-assemble into icosahedral crystals. Colloidal volume fractions of 1, 2 and 3 % were tested (figure 4.14). Most icosahedral supraparticles had a diameter of approximately 10  $\mu\text{m}$  and occurred the most using a 2 and 3 v/v% of titania-silica composites (figure 4.14 A & B). The supraparticles in the 1 v/v% sample seemed to aggregate (figure 4.14A). The synthesis methods were exactly the same, so the reason is unclear. The general consensus was that the 2 and 3 v/v% of colloids yielded the best icosahedral supraparticles.

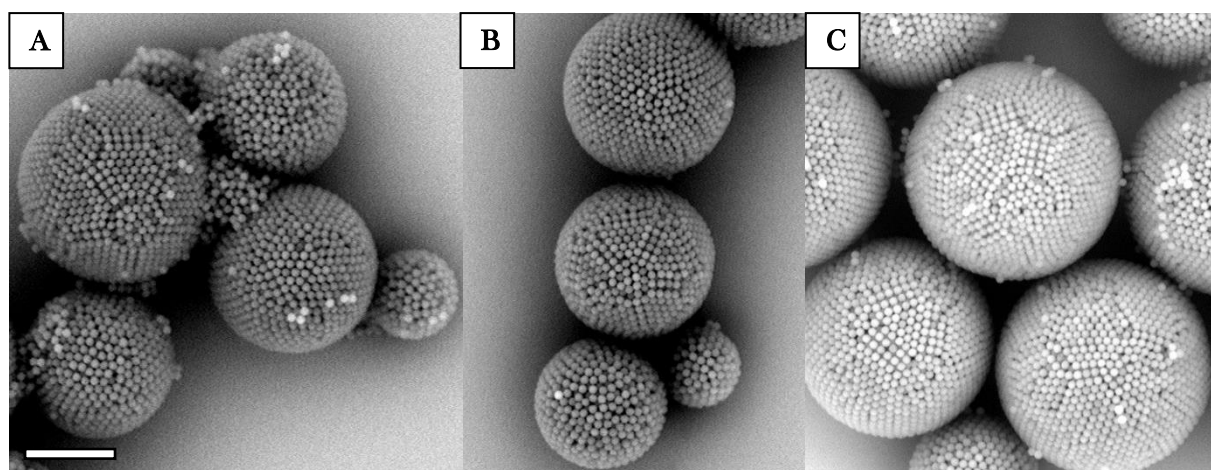


**Figure 4.14:** SEM images of icosahedral supraparticle samples with different colloid volume fractions inside the emulsion droplets. (Scale bar: 5  $\mu\text{m}$ ) (a) Supraparticles formed with 1 v/v % of colloids (b) Supraparticles formed with 2 v/v% of colloids (c) Supraparticles formed with 3 v/v% of colloids.

In all icosahedral supraparticle samples there were also onion-shaped or mixed supraparticles in the same size range as the icosahedral supraparticles (figures 4.14, 4.15A). The only explanation for this is that the size of the emulsion droplet and the location within the glass vial were also important for the formation of the icosahedral structure. Possibly a location closer to the glass vial bottom surface and a larger emulsion droplet could allow slower spatial confinement giving these supraparticles more time to

assemble in icosahedral crystals. The samples containing icosahedral supraparticles also showed bright iridescent colours when illuminated with a broad spectrum pen light. Figure 4.15B shows an optical image of possibly two icosahedral shaped supraparticles, the exact crystal structure couldn't be determined with the optical microscope. The optical image does differ greatly from a pure onion-shaped supraparticle (figure 4.12B), showing a more patterned light and brighter colours. However, a bow-tie pattern as described by Kim et al. (2020)<sup>4</sup> is not discernible. Therefore, it is not entirely certain if the image depicts the icosahedral shaped supraparticles. Figure 4.15D shows the inner structure of probably an icosahedral supraparticle since on the right hand side Mackey cores and Anti-Mackey edges can be distinguished. However, the left-hand side resembles the inside structure of an onion-shaped supraparticle. It is unclear if this is just an effect of the way that the supraparticle is broken or if the supraparticle contained a mixture of onion-shaped and icosahedral structures.

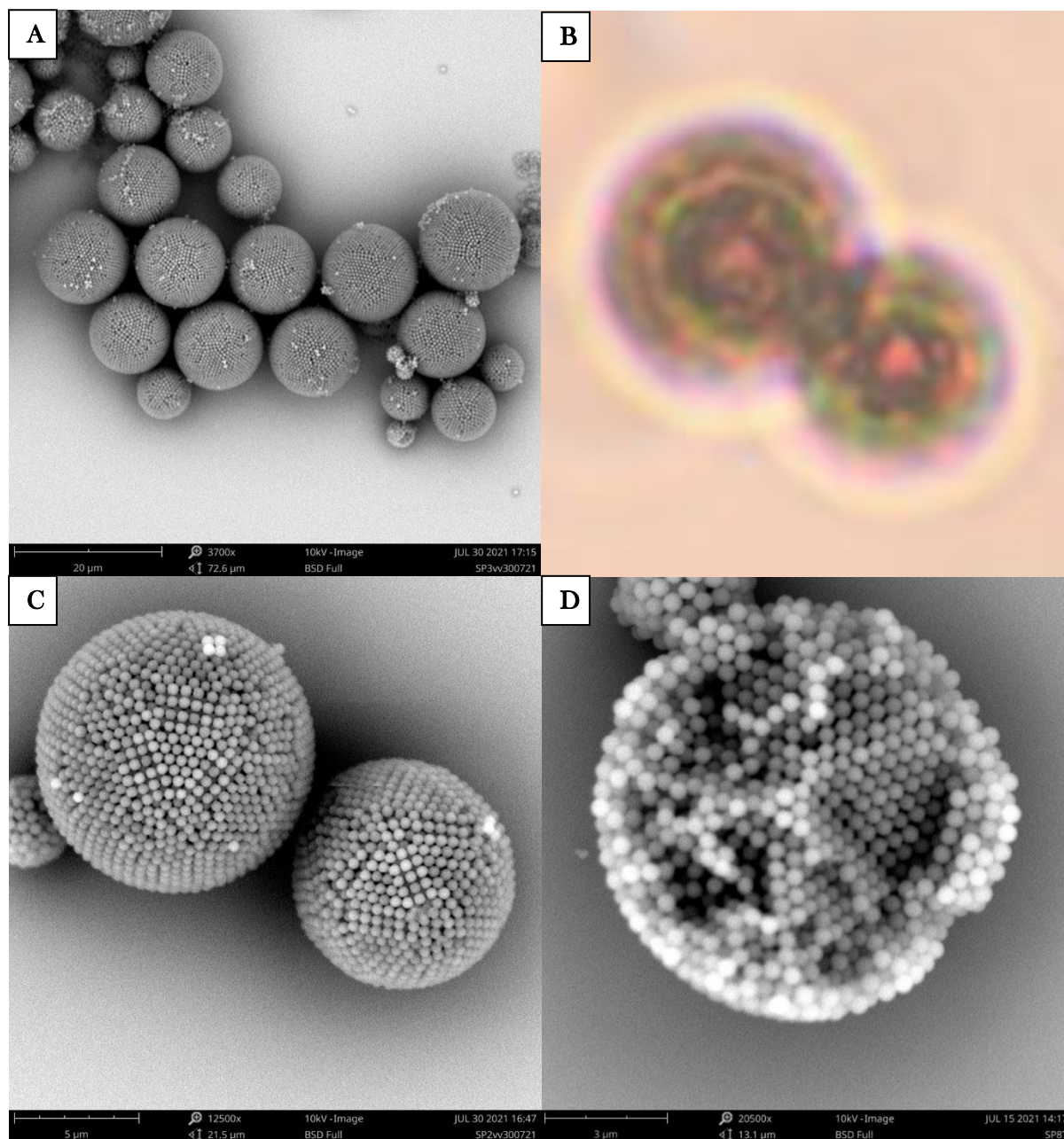


**Figure 4.15:** SEM images of icosahedral and onion shaped supraparticles. (a) Overview of differently sized supraparticles with icosahedral and onion shaped structure. (b) Optical microscope image of possibly two icosahedral shaped supraparticles. (c) Two icosahedral shaped supraparticles with diameter of 11.1  $\mu\text{m}$  and 9.1  $\mu\text{m}$ , respectively. (d) SEM image of a broken supraparticle with a diameter of 10.5  $\mu\text{m}$ , showing an ordered, possibly Mackey core, structure within the supraparticle.

#### 4.4.2 Oil in water

In the first experiment, the OTMOS coated titania-silica composites (figure 4.8) were dispersed in cyclohexane (2 v/v %) and emulsified in cyclohexane saturated water in a 20 mL glass vial with 2 layers of Teflon tape and a single 0.9 mm hole. After two days of drying the supraparticles were imaged with a SEM microscope (figure 4.16). Because evaporation went too fast, the colloids looked to have the tendency to assemble in polyhedron-like structures.

An exactly similar sample was additionally sonicated for 5 minutes after shaking the sample by hand to form the emulsion droplets, this was done with the intention to create smaller and more evenly distributed emulsion droplets in the sample. In general, the extra sonication step seemed to result in more deformed supraparticles (figure 4.17). The emulsion droplets could possibly have become too small and therefore evaporated too fast to enable structured self-assembly.

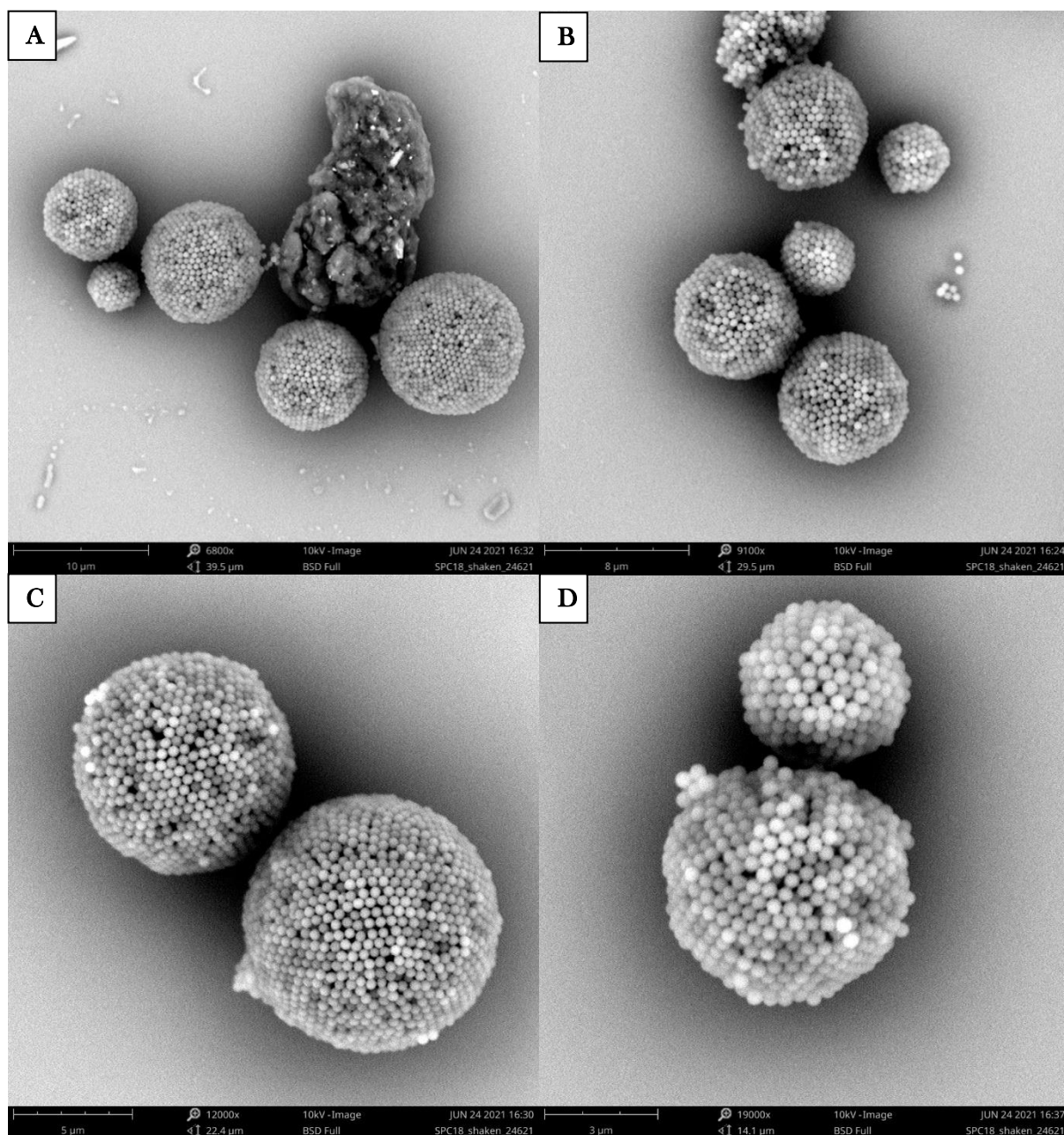


**Figure 4.16:** Supraparticles formed with OTMOS coated titania-silica composites when emulsion droplets evaporate too fast. (a) Diameters of the supraparticles from left to right are roughly 6.9, 3.9, 8.8, 8.3 and 10.7  $\mu\text{m}$ . (b) Diameters of the supraparticles from top to bottom are roughly 6.8, 3.7, 3.8, 6.7 and 7.1  $\mu\text{m}$ . (c) Diameters of the supraparticles from left to right are roughly 9.1 and 10.8  $\mu\text{m}$ . (d) Diameters of the supraparticles from top to bottom are roughly 4.5 and 6.5  $\mu\text{m}$ .



Because cyclohexane evaporates faster than water due to its lower boiling point, together with the larger size of the colloids (506 nm vs 421 nm) this meant that evaporation was generally too fast to form perfect crystalline structures. Another differing factor from the water in oil supraparticles is that the cyclohexane emulsion droplets float on the top of the solvent surface whereas the water emulsion droplets sediment. The direct contact to air could possibly enhance the evaporation even further. The most uniform onion-shaped structured supraparticles were formed with a 5 v/v % dispersion of OTMOS coated titania-silica composites and a 20 mL glass vial closed off with a septum stopper covered in Teflon tape and a single 0.4 mm \* 19 mm Microlance needle struck through the top (figure 4.18). These supraparticles did however not show clear iridescence when shining a broad spectrum pen light through the sample, as was also observed in optical images taken from the supraparticles (figure 4.18B). This did not come as a complete surprise since the colloids also did not show any iridescence. An onion-shaped inner structure could be seen in the broken particles (figure 4.18D).

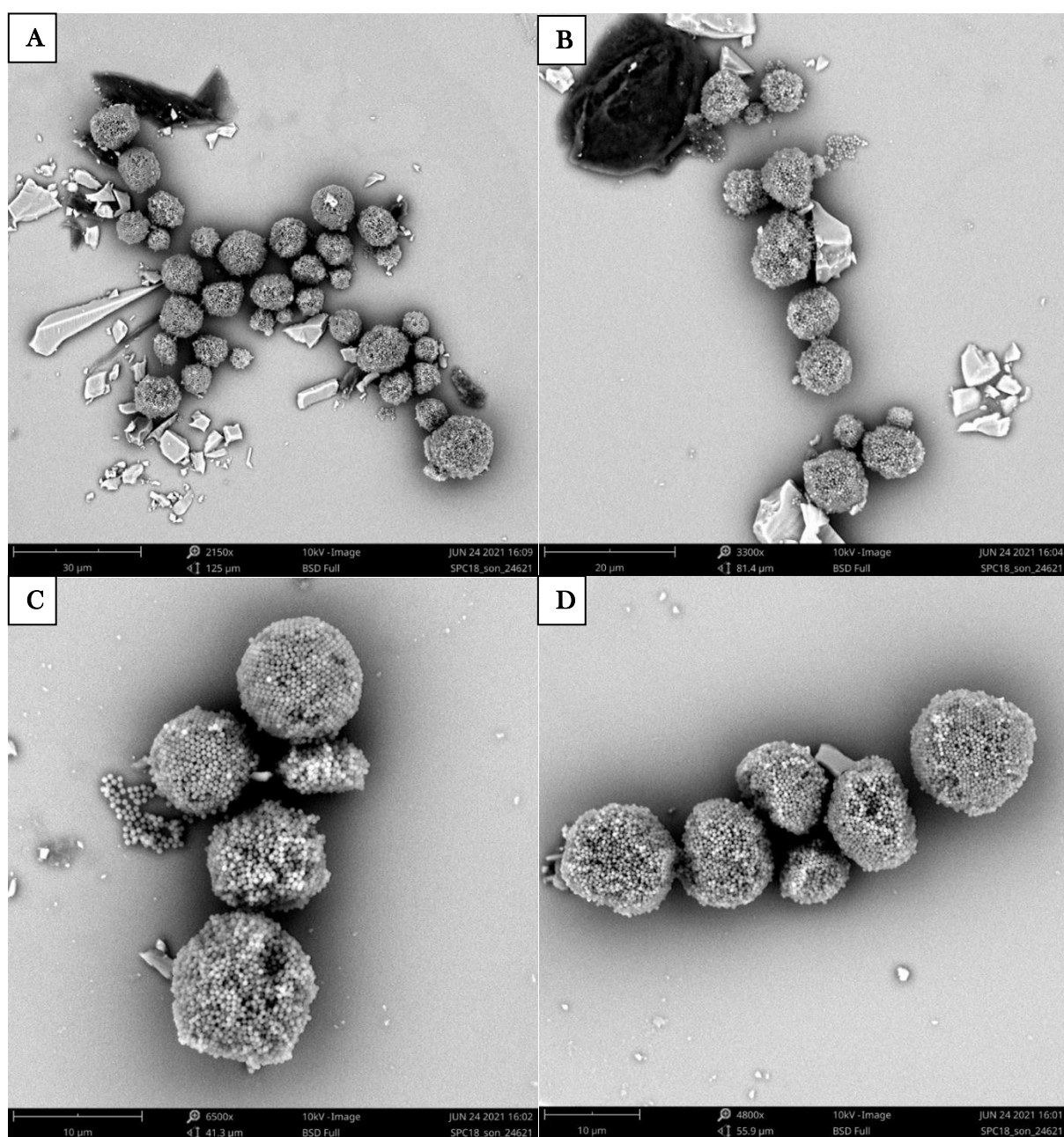


**Figure 4.17:** Supraparticles formed with OTMOS coated titania-silica composites when the sample was additionally sonicated for 5 minutes before drying of the droplets. Almost none of the supraparticles are spherical in shape.

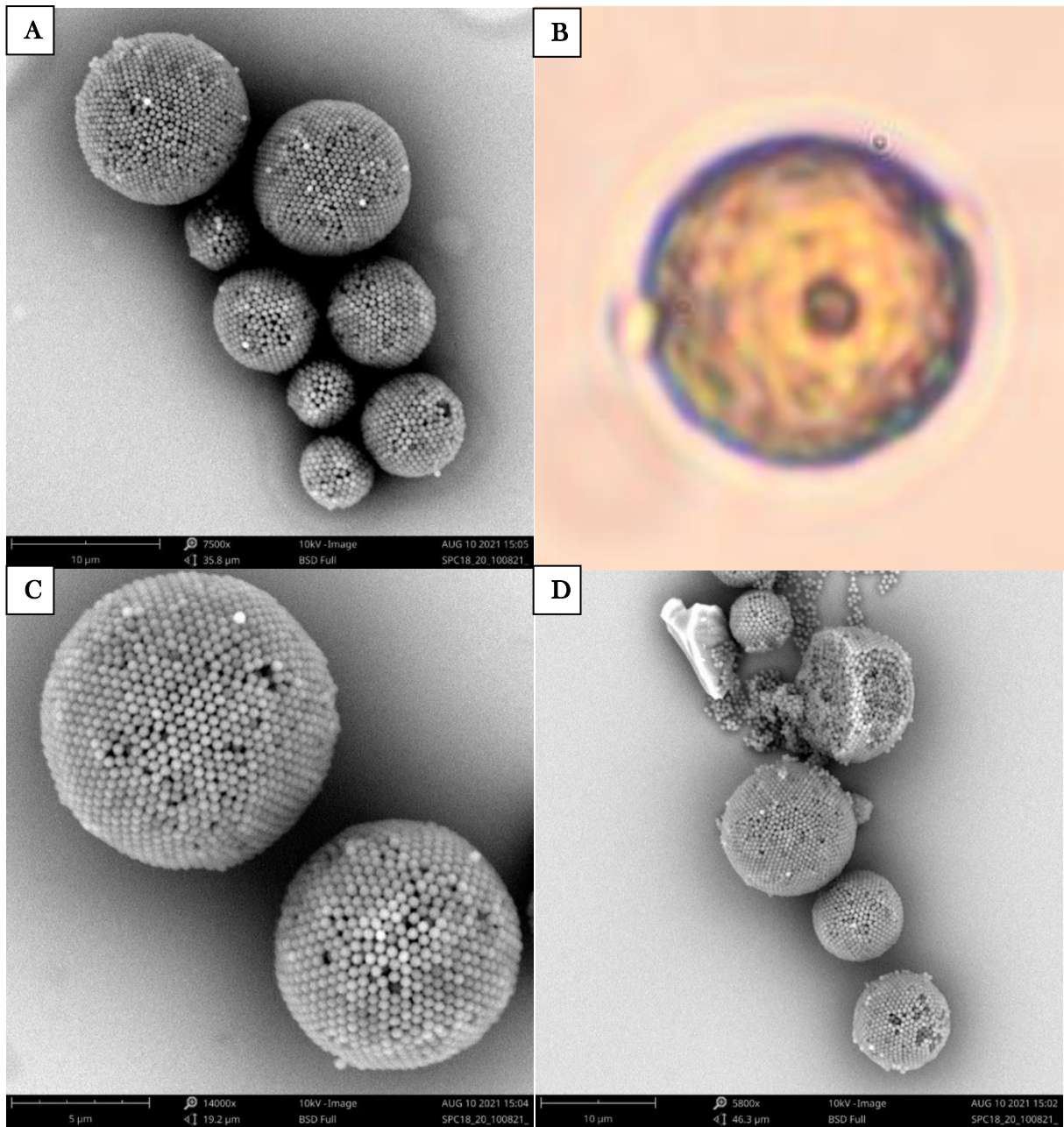


**Figure 4.18:** Onion-shaped supraparticles formed with OTMOS coated titania-silica composites. (a) Different sizes of supraparticles. Diameter from top to bottom: 11.8 μm, 10.7 μm, 4.7 μm, 7.6 μm, 7.1 μm, 4.3 μm, 7.2 μm and 5.2 μm. (b) Optical image of one of the supraparticles. (c) Two onion-shaped supraparticles with a diameter of 10.8 and 9.2 μm, respectively. (d) Broken supraparticle showing the inside structure of the supraparticles.

## 5 Conclusion and outlook

In this report we showed the successful synthesis of monodisperse amorphous titania colloids with an average diameter size of 438 nm and polydispersity of 6%. Silica coating of these colloids resulted in the stable 421 nm monodisperse (3%) titania-silica composites that were able to self-assemble into onion-shaped and icosahedral supraparticles through evaporation-induced spherical confinement. Parameters such as evaporation rate, solvents used and colloid size proved to have a large role in the rate of assembly. It was found that icosahedral structures could be formed in a water-hexadecane emulsion using 7 mL vials, two layers of Teflon tape and only a single hole of 0.4 mm diameter. These structures also seemed to show brighter colours than their onion-shaped counterparts when shining a broad spectrum penlight through the sample. The only alteration necessary to form onion-shaped supraparticles was to switch the 7 mL vial with a 20 mL one. This vial has a larger diameter and volume meaning that the most likely explanation for the difference in crystallinity would be the increased liquid-air surface area which could cause slightly faster evaporation of the water emulsion droplets, this is in accordance with the paper from *Kim et al.* (2020)<sup>4</sup>. However, the time needing to dry the droplets was on a whole other scale than mentioned in the paper of *Kim et al.* (2020), where they mentioned to have onion-shaped supraparticles within 20 minutes and icosahedral shaped ones within 7 hours. We found that the supraparticle samples were typically dry enough for washing after 8 to 14 days. Since the time scale to diffuse over ones own diameter scales with  $R^3$ , an increasing factor of  $(450/300)^3$ , which is 3.375, was to be expected but not the 8 to 14 days we observed. Washing and imaging the samples before 8 days typically destroyed the supraparticles, because they were not assembled or stable yet, or resulted in amorphous supraparticles (figure 4.11). Reasons for this vastly different timeframe are unknown, the difference in colloid size does not seem to be the problem here since similar experiments with smaller colloids performed by others in the group, yielded the same results. However, a different technique in producing the emulsion droplets was used, so it might be that the size of the emulsion droplets also plays a large role in this self-assembly process.

The titania-silica composites were also coated with OTMOS, which made them lose their iridescence. Particles will lose their iridescent properties when the volume fractions of the titania becomes below 55%. Where one would expect a maximum layer of 10 nm OTMOS coating due to its C18 chains, a layer of around 40 nm or more was typically found. This begs the question if the OTMOS in combination with the titania-silica composites somehow causes the colloids to swell slightly. Another possibility could be that the calibration of the TEM microscope varies slightly between the different pictures. Further analysis of these OTMOS coated colloids is needed to confirm the exact cause. The OTMOS coated titania-silica composites, were more difficult to assemble compared to the uncoated colloids. Mostly due to the decreasing speed of self-assembly for bigger colloids<sup>25</sup>, but also because of the lower boiling point of cyclohexane (81 °C), the chosen discontinuous phase in the water-cyclohexane emulsion. These two reasons combined ensured that the evaporation rate couldn't be slowed down enough to form highly structured supraparticles, but semi onion-shaped supraparticles were formed using 7 and 20 mL vials and four layers of Teflon tape with a single hole of 0.4 mm diameter. These supraparticles could likely be improved using different solvents with higher boiling points, by reducing the diameter of the individual colloids or lowering of temperature during incubation.

There are still many experiments that could be conducted to try to reduce the size of the original titania colloids. First of all, it should be possible to reduce the pores of the titania colloids without losing the uniformity of the colloids. Maybe by autoclaving the sample or increasing the pressure on the individual colloids with repulsive forces could accomplish this. Furthermore, parameters within the synthesis method could be tweaked or expanded such that smaller monodisperse titania colloids can be formed. Lastly, a different titania colloid synthesis method could be performed, such as the solvothermal or one of the templated techniques, to improve the crystallinity of the colloids and decrease their size.

Since apparently the titania-silica composites used in the supraparticle experiments did not really have a silica layer it could still be interesting to observe the effects if there was. A thicker silica layer could be applied to the composites or if the crystallinity of the titania is improved it might be possible to form a homogeneous silica layer around the titania colloids. If this succeeds the effects of OTMOS coating would also be easier to determine and functionalisation of the colloids with FITC might result in less aggregates. If supraparticles with FITC colloids could be made, confocal microscopy might yield clearer images of the inside structure of the supraparticles. We will not have to deal with the light scattering of the titania in the reflection channel but can instead look at the fluorescent signals.

Finally, it would also be interesting to improve the supraparticle synthesis to produce more monodisperse supraparticles with the same crystal structures. Steven Remiëns showed in his bachelor thesis<sup>49</sup> that by using microfluidics to form monodisperse emulsion droplets the resulting supraparticles were also more monodisperse. Improving this technique and adjusting the parameters to fit this colloidal system has high potential for more controlled supraparticle assembly, possibly making the technique suitable to create crystalline supraparticles in bulk.

To conclude, we showed that it is possible to create photonic crystals out of titania colloids. It would be interesting to perform more experiments with these supraparticles, such as applying a carbon shell to enhance the structural colours<sup>4</sup>, or a more advanced optical analysis to determine the exact properties of the supraparticles. These supraparticles show great potential and could eventually be useful in a whole range of applications, from structural colours to catalysis reactions and are therefore worthwhile to investigate further.

## 6 Materials and methods

### 6.1 Chemicals and materials

All chemicals used in the experiments were extracted directly from the ordered flasks available in the lab and not altered in any way. The used chemical were: Methanol (ACS reagent,  $\geq 99.8\%$ , Sigma-Aldrich no. 32213), acetonitrile (99.8%, Sigma-Aldrich no. 271004), dodecylamine (DDA, Merck no. 8.03527.0500), Titanium (IV) isopropoxide (TTIP,  $\geq 97.0\%$ , Sigma-Aldrich no. 87560), ethanol absolute (EtOH, 100v%, Supelco no. 1.00983.2500), ammonium hydroxide solution (p.a.  $\sim 25\%$   $\text{NH}_3$  basis, Sigma-Aldrich no. 30501), tetraethyl orthosilicate (TEOS, reagent grade, 98%, Sigma-Aldrich no. 131903), Fluorescein isothiocyanate isomer I (FITC,  $\geq 90\%$ , Sigma-Aldrich no. F7250), (3-aminopropyl)triethoxysilane (APS,  $\geq 98\%$ , Sigma-Aldrich no. A3648), octadecyltrimethoxysilane (OTMOS, technical grade, 90%, Sigma-Aldrich no. 376213), toluene (SupraSolv no. 1.08389.2500), butylamine (99.5%, Sigma-Aldrich no. 471305), n-hexadecane (99%, Alfa Aesar no. A10322), hypermer™ 2296-LQ-(MV) (Croda, batch no. 0001693192), ultrapure (type 1) water (Direct-Q 3), hexane (<5% n-Hexane, Honeywell | Riedel-de Haën™ no. 34484), sodium dodecyl sulfate (SDS, ACS reagent,  $\geq 99.0\%$ , Sigma-Aldrich no. 436143) and cyclohexane (LiChrosolv no. 1.02827.2500).

All glassware and materials used in the experiments were cleaned with 96% ethanol before and after use. Glassware was additionally washed with soap and hot water after use.

All experiments were conducted under room temperature unless mentioned otherwise.

### 6.2 Amorphous titania colloid synthesis

A sol-gel method described by Schertel et al. (2019)<sup>20</sup> was used for the titania colloid synthesis. 106.00 mL methanol was mixed with 42.00 mL acetonitrile and stirred in a three-necked round-bottom flask at 500 rpm. Next, 1.00 g (5.4 mmole) of dodecylamine (DDA) was added to the solvent and stirred for 5 minutes. After the DDA was dissolved, 700  $\mu\text{L}$  (39 mmole) purified water was added to the middle of the mixture and stirred for 10 more minutes. The flask was closed off by a septum stopper and a glass stopper with Keck clip, the third neck was connected to a continuous nitrogen flow to allow for a nitrogen environment. After these 10 minutes of stirring, 1.000 mL (3.4 mmole) of Titanium (IV) isopropoxide (TTIP) precursor was instantly added to the mixture under vigorous stirring and a nitrogen environment. As TTIP precursor is moisture sensitive, it must be handled in a glovebox under an inert atmosphere, to minimise exposure to water and oxygen. Therefore, a syringe of 1.000 mL was prepared beforehand in the glovebox and sealed with a septum. The reaction mixture was stirred at 300 Revolutions Per Minute (rpm) overnight for 16 hours (Appendix figure 4). The synthesized colloids were then divided in 4, 50 mL Eppendorf tubes and washed three times with methanol by centrifuging at 300 Relative Centrifugal Force (RCF) for 15 min for each washing step. Between washing steps, the colloids were sonicated to redisperse them in the methanol. After the final washing step, the colloids were stored in methanol in a 20 mL glass vial.

#### 6.2.1 Titania condensation experiments

Three different heating experiments were performed to attempt to condense the synthesized titania colloids (figure 4.3). The aim was to increase the titania density and make the colloids more compact, while maintaining the spherical shape and monodispersity of the colloids.

In the first heating experiment, 113.7 mg titania colloids were dispersed in 50 mL purified water with 1.00 mL ammonium hydroxide solution in a closed off round-bottom flask. The colloids were then heated to

80 °C and stirred at 300 rpm for 65 hours. After a single washing step by centrifuging at 300 RCF for 15 minutes, the colloids were redispersed through sonication and stored in methanol.

In a second heating experiment, ≈250 mg titania colloids dispersed in methanol were deposited on an aluminium foil bowl and placed under a heat lamp for 30 minutes. The colloids were then redispersed in methanol and placed in a sonicator for another 30 minutes before storing the sample.

In the third heating experiments, 111.7 mg titania colloids were dispersed in 50.00 mL methanol in a round-bottom flask closed off with a glass stopper, a Keck clip and vacuum grease. The solution was then heated to 40 °C and stirred at 300 rpm for 19 hours. Next, the colloids were washed with methanol by centrifuging 2 times at 300 RCF for 15 min and the supernatant was centrifuged an additional 15 min at 500 RCF. The sediments were together redispersed through sonication and stored in methanol.

### 6.3 Silica coating of the titania colloids<sup>50</sup>

A single silica layer was added to the titania colloids through seeded Stöber growth. The colloids were first centrifuged (300 RCF, 15 min) and redispersed in 50.00 mL of absolute ethanol. Next, 0.550 mL (14 mmole) ammonium hydroxide solution was added to the mixture and put in a single-necked round-bottom flask. The flask was sonicated for 15 minutes to ensure complete dispersion of the titania colloids. The flask was put on a stirrer and under vigorous stirring (500 rpm) a calculated amount of tetraethyl orthosilicate (TEOS) was added to the mixture, see formula 1 below. Since most synthesized titania colloids had a diameter around 450 nm this generally resulted in 1.500 mL (6.7 mmole) TEOS being added per 100 mg of titania colloids.

$$\#TEOS * C = V_s * \#P = \frac{4}{3} \pi (r_s^3 - r_t^3) * \frac{m}{\rho_t * \frac{4}{3} \pi r_t^3} \quad (1)$$

**Formula 1:** Where  $\#TEOS$  is the amount of TEOS to add in mL,  $C$  the correction factor for the experiment, in this case 0.0247 which is obtained from previous experiments,  $V_s$  the volume of the silica layer per colloid,  $\#P$  is the total number of titania colloids,  $r$  the (desired) radius of the colloid with a 50 nm silica layer and  $r_t$  the radius of the titania colloids in cm,  $m$  the amount of titania colloids in grams and  $\rho$  the density of the titania colloids, set at 2.5 g/cm<sup>3</sup>. Radius of the colloids is determined by TEM image analysis.

The reaction mixture was stirred overnight at 300 rpm for 21 hours. Then the mixture was divided in two 50 mL Eppendorf tubes and washed three times with absolute ethanol by centrifuging at 500 RCF for 15 min for each washing step. Between washing steps the colloids were redispersed through sonication of the sample. After washing, the colloids were stored in absolute ethanol in a 7 mL glass vial.

#### 6.3.1 Fluorescein isothiocyanate (FITC) functionalisation

In some experiments a fluorescent layer was added to the silica layer of the colloids. In this case a dye mixture was prepared by adding 2.60 mg (6.7 μmole) of fluorescein isothiocyanate (FITC) to 1.000 mL of absolute ethanol and stirring for 15 min. Next, 16.0 μL (67 μmole) of (3-aminopropyl)triethoxysilane (APS) was added to the mixture in a 1:10 FITC:APS molar ratio and the vial was covered with aluminium foil and left to stir for another 24 hours.

The dye mixture was added to the Stöber reaction mixture directly after the TEOS for the first 50 nm silica layer. After 24 hours of stirring at 300 rpm, another 0.550 mL (14 mmole) ammonia for a second 10 nm silica layer (without dye) was added to the colloids by drop-wise injecting another pre-calculated amount of TEOS (dissolved in 1.000 mL absolute ethanol) to the reaction mixture under vigorous stirring. After 4 hours of stirring at 300 rpm the sample was washed in the same manner as described in part 6.3.

## 6.4 Octadecyltrimethoxysilane (OTMOS) functionalisation<sup>42</sup>

To functionalize the silica coated titania colloids with OTMOS, a small amount of colloids were centrifuged at 500 rpm after which the supernatant was removed. The sediment was further dried carefully with nitrogen gas. Next, 76.00  $\mu\text{L}$  (718  $\mu\text{mole}$ ) toluene, 7.600  $\mu\text{L}$  (77  $\mu\text{mole}$ ) butylamine and 7.600  $\mu\text{L}$  (18  $\mu\text{mole}$ ) OTMOS in a 10:1:1 volume ratio was added per 10 mg of colloids. These amounts were determined by calculating the amount of OTMOS molecules able to bind to the surface of one colloid, provided that the grafting density is around 0.3 molecules/ $\text{nm}^2$ . The mixture was then sonicated for 4 hours. After sonication the sample was washed first with toluene, then three more times with cyclohexane by centrifuging at 500 RCF for 10 min for each washing step. The sample was stored in cyclohexane in a glass vial.

## 6.5 Supraparticle formation

### 6.5.1 Water in oil emulsion<sup>4</sup>

For the water in oil emulsion 10.00 mL hexadecane was first mixed with 3 w/w % (231.0 mg) hypermer™ 2296-LQ-(MV) and then stirred and heated to 50 °C. At 50 °C the hexadecane was saturated by adding 1.000  $\mu\text{L}$  purified water per 1.000 mL hexadecane. The mixture was stirred at 450 rpm and heated for 20 min after which it was set aside to cool down to room temperature. It was important to do a new hexadecane saturation before the start of each new sample. Next, 2.000 mL of the hexadecane was pipetted into a glass vial (20 mL vial for onion shaped and 7 mL vial for icosahedral shaped supraparticles) and 25.00  $\mu\text{L}$  of 2-3 v/v % of silica coated titania colloids dispersed in purified water were slowly added to the hexadecane mixture by pipetting just below the surface and to the side of the vial. Quickly after pipetting the sample was shaken vigorously by hand for 3 seconds after which the cap was replaced by two layers of Teflon tape with a single hole made by a 0.4 mm \* 19 mm Microlance needle to allow evaporation of the sample. The sample was then placed on a IKA KS 260 basic shaker at 250 rpm for 1-2 weeks or until the water had evaporated, no shaking by hand in the meantime. The supraparticles were then washed three times with hexane by centrifuging at 50 RCF for 15 min for each washing step.

### 6.5.2 Oil in water emulsion<sup>50</sup>

For the oil in water emulsion 28.0 mg (97  $\mu\text{mole}$ ) of sodium dodecyl sulfate (SDS) was added per 5.00 mL of purified water. To saturate the water, cyclohexane was added to the water/SDS mixture, shaken, and left to settle. Then, 2.000 mL of the bottom layer was removed and put in a clean glass vial. 25.00  $\mu\text{L}$  of 1-5 v/v % OTMOS coated titania-silica colloids was slowly added to the mixture and vigorously shaken by hand for 3 seconds. The cap was then replaced by a septum stopper covered in Teflon tape and a single 0.4 mm \* 19 mm Microlance needle was struck through the top. The sample was placed on a IKA KS 260 basic shaker at 250 rpm for ~48 hours or until the cyclohexane had evaporated. The supraparticles were then washed three times with purified water by centrifuging at 50 RCF for 15 min for each washing step.

## 6.6 Microscopes used

Multiple microscopes were used for the imaging of the particles. Below you find the sample preparation, settings and types of microscopes used for imaging.

### 6.6.1 Confocal imaging

A Leica TCS SP8 STED microscope with a 63x/1.30 HC PL APO CS2 glycerol confocal objective and a 1.21 AU pinhole was used for confocal imaging. A 80 MHz pulsed white light laser (SuperK, NKT Photonics) with an excitation wavelength set to 488 nm at 50% laser power was used during imaging of the sample. Reflective signals were detected with a photomultiplier tube (PMT) detector at wavelengths between 478 nm and 498 nm, 10 nm apart from the excitation wavelength. Fluorescent signals were detected with a HyD detector at wavelengths between 509 nm and 623 nm. Scanning speed, zoom factor, gain and resolution were adjusted per sample to obtain the best images. Images were typically taken with a resolution of 512 px x 512 px and a pixel size varying between 160 nm - 10 nm.

The confocal samples were prepared on a simple microscope glass slide (Appendix figure 5). A Vitrotube glass capillary of 0.1\*1.0 mm from VitroCom was used to collect the sample and glued with UV glue (Norland Optical Adhesive 68) to the glass slide at the tips. Subsequently, the sample was placed under a long wave UV lamp for approximately 3 minutes to harden the glue.

### 6.6.2 Scanning Electron Microscopy (SEM) imaging

A Phenom ProX Desktop SEM with a standard sample holder was used for Scanning Electron Microscopy (SEM) imaging. The following settings were used: mode: high res. (10kV), intensity: image, detector: BSD Full, resolution: 1024 and quality: high. Auto focus and lighting/contrast were used before acquiring images.

The SEM samples were prepared by pipetting 20  $\mu$ L of the sample onto a piece of silicon wafer. The silicon wafer was then placed under a heating lamp until all liquids were evaporated. When dry, the silicon wafer was then attached to an aluminium SEM specimen stub with a conductive carbon tape sticker.

### 6.6.3 Transmission Electron Microscopy (TEM) and Energy Dispersive X-Ray (EDX) imaging

A Tecnai F20 TEM was used for Transmission Electron Microscopy (TEM) imaging. TEM images were used to investigate the shape and the diameter of the synthesized colloids. By checking the size of the colloids, the polydispersity was obtained for each sample.

Energy Dispersive X-Ray (EDX) images were provided using a FEI Talos F200X S/TEM. The EDX images were used to determine the composition of the synthesized colloids.

The TEM samples were prepared on a Formvar/Carbon 200 mesh CU TEM grid by pipetting 4-5  $\mu$ L of the sample onto the grid. The grids were placed in sterile plastic caps and covered with parafilm after pipetting to allow slow drying of the sample (Appendix figure 5).

## 6.7 Polydispersity calculation

The average diameter and polydispersity of the colloids were calculated using a python script provided by Maarten Bransen on the TEM images (Appendix 10.5). The formula used to calculate the polydispersity of the colloids in % was:  $PD = 100 * Std(diameter) / Mean(diameter)$ . When contrast between background and colloids was too low the script didn't work as well, in this case diameters were manually measured in Fiji with a minimum of 100 measurements to calculate the average diameter and polydispersity.



## 7 Acknowledgements

I would of course like to thank my daily supervisor Zahra Peimanifard for being a huge support, making all the TEM images of my particles and always being there to explain the experiments to me. Zahra provided me with all the information I needed to know and helped me on my way at each step of the project.

Special thanks also go to: My supervisor Alfons van Blaaderen, who always gave good feedback and offered tons of good follow-up experiments for my project. Maarten Bransen, who provided me with and taught me the python code to determine the polydispersity of my colloids and also taught me how to use the confocal microscope. Furthermore he was always ready to answer my questions and help me with my problems. Roy Hoitink, for being a major help with all supraparticle related experiments and who kindly explained to me how to prepare SEM samples and even took SEM images for me when the Phenom microscope was temporarily out of order. Kelly Brouwer, for being so kind to make EDX images of my colloids. And Chris Schneijdenberg, for teaching me how to use the Phenom ProX.

I also want to thank all the other members in the Soft Condensed Matter group for always being prepared to help and give feedback in the informal group meetings. Your hospitality and good remarks have helped me feeling welcomed and valued in the group.

## 8 Bibliography

1. Team - Exploration Architecture. Available at: <http://exploration-architecture.com/studio/team>. (Accessed: 25th October 2021)
2. biomimicry KTH: Biomimicry in architecture and the start of the Ecological Age. Available at: <http://biomimicrykth.blogspot.com/2012/05/biomimicry-in-architecture-and-start-of.html>. (Accessed: 28th July 2021)
3. Wang, J. *et al.* Structural Color of Colloidal Clusters as a Tool to Investigate Structure and Dynamics. *Adv. Funct. Mater.* **30**, 1907730 (2020).
4. Kim, C. *et al.* Controlled assembly of icosahedral colloidal clusters for structural coloration. *Chem. Mater.* **32**, 9704–9712 (2020).
5. Vogel, N. *et al.* Color from hierarchy: Diverse optical properties of micron-sized spherical colloidal assemblies. *Proc. Natl. Acad. Sci.* **112**, 10845–10850 (2015).
6. Ding, Y. *et al.* Nanoporous TiO<sub>2</sub> spheres with tailored textural properties: Controllable synthesis, formation mechanism, and photochemical applications. *Prog. Mater. Sci.* **109**, 100620 (2020).
7. Cargnello, M., Gordon, T. R. & Murray, C. B. Solution-Phase Synthesis of Titanium Dioxide Nanoparticles and Nanocrystals. *Chem. Rev.* **114**, 9319–9345 (2014).
8. Chen, X. & Mao, S. S. Titanium Dioxide Nanomaterials: Synthesis, Properties, Modifications, and Applications. *Chem. Rev.* **107**, 2891–2959 (2007).
9. Chen, D. & Caruso, R. A. Recent Progress in the Synthesis of Spherical Titania Nanostructures and Their Applications. *Adv. Funct. Mater.* **23**, 1356–1374 (2013).
10. Cargnello, M., Gordon, T. R. & Murray, C. B. Solution-Phase Synthesis of Titanium Dioxide Nanoparticles and Nanocrystals. *Chem. Rev.* **114**, 9319–9345 (2014).
11. Matijević, E., Budnik, M. & Meites, L. Preparation and mechanism of formation of titanium dioxide hydrosols of narrow size distribution. *J. Colloid Interface Sci.* **61**, 302–311 (1977).
12. Chemseddine, A. & Moritz, T. Nanostructuring titania: Control over nanocrystal structure, size, shape, and organization. *Eur. J. Inorg. Chem.* 235–245 (1999). doi:10.1002/(sici)1099-0682(19990202)1999:2<235::aid-ejic235>3.0.co;2-n
13. Hermann Möckel, Michael Giersig & Frank Willig. Formation of uniform size anatase nanocrystals from bis(ammonium lactato)titanium dihydroxide by thermohydrolysis. *J. Mater. Chem.* **9**, 3051–3056 (1999).
14. Liu, L. *et al.* Anion-Assisted Synthesis of TiO<sub>2</sub> Nanocrystals with Tunable Crystal Forms and Crystal Facets and Their Photocatalytic Redox Activities in Organic Reactions. *J. Phys. Chem. C* **117**, 18578–18587 (2013).
15. Min-Han Yang *et al.* Alkali metal ion assisted synthesis of faceted anatase TiO<sub>2</sub>. *CrystEngComm* **15**, 2966–2971 (2013).
16. Jimin Du, Jiangshan Zhang & Joon Kang, D. Controlled synthesis of anatase TiO<sub>2</sub> nano-octahedra and nanospheres: shape-dependent effects on the optical and electrochemical properties. *CrystEngComm* **13**, 4270–4275 (2011).
17. Buonsanti, R. *et al.* Nonhydrolytic Synthesis of High-Quality Anisotropically Shaped Brookite TiO<sub>2</sub> Nanocrystals. *J. Am. Chem. Soc.* **130**, 11223–11233 (2008).
18. Wang, Z. & Lou, X. W. (David). TiO<sub>2</sub> Nanocages: Fast Synthesis, Interior Functionalization and

- Improved Lithium Storage Properties. *Adv. Mater.* **24**, 4124–4129 (2012).
19. Kim, K. Do, Kim, S. H. & Kim, H. T. Applying the Taguchi method to the optimization for the synthesis of TiO<sub>2</sub> nanoparticles by hydrolysis of TEOT in micelles. *Colloids Surfaces A Physicochem. Eng. Asp.* **254**, 99–105 (2005).
  20. Schertel, L. *et al.* Tunable high-index photonic glasses. *Phys. Rev. Mater.* **3**, 015203 (2019).
  21. Velev, O. D., Furusawa, K. & Nagayama, K. Assembly of latex particles by using emulsion droplets as templates. 1. Microstructured hollow spheres. *Langmuir* **12**, 2374–2384 (1996).
  22. Montanarella, F. A self-Assembly Tale: Collective structural and optical phenomena in supraparticles of nanocrystals. *PhD Thesis* (Soft Condensed Matter group, Utrecht University, 2019).
  23. Wang, D. Quantitative Real-space Analysis of Colloidal Supraparticles Self-assembled from Monodisperse Nanoparticles. *PhD Thesis* (Soft Condensed Matter group, Utrecht University, 2018).
  24. Wintzheimer, S. *et al.* Supraparticles: Functionality from Uniform Structural Motifs. *ACS Nano* **12**, 5093–5120 (2018).
  25. de Nijs, B. Towards Crystals of Crystals of NanoCrystals: A Self-Assembly Study. *PhD Thesis* (Soft Condensed Matter group, Utrecht University, 2014).
  26. Jiang, Y. fan, Zheng, A., Zheng, S. jian, Liu, W. ming & Zhuang, L. Amorphous photonic structures with high reflective index based on incorporating Fe<sub>3</sub>O<sub>4</sub>@SiO<sub>2</sub> core/shell colloidal nanoparticles into silica nanospheres. *J. Appl. Phys.* **128**, 103106 (2020).
  27. Rong, X. *et al.* Liquid marble-derived solid-liquid hybrid superparticles for CO<sub>2</sub> capture. *Nat. Commun.* **10**, 1854 (2019).
  28. Wenderoth, S., Granath, T., Prieschl, J., Wintzheimer, S. & Mandel, K. Abrasion Indicators for Smart Surfaces Based on a Luminescence Turn-On Effect in Supraparticles. *Adv. Photonics Res.* **1**, 2000023 (2020).
  29. Müssig, S. *et al.* Supraparticles with a Magnetic Fingerprint Readable by Magnetic Particle Spectroscopy: An Alternative beyond Optical Tracers. *Adv. Mater. Technol.* **4**, 1900300 (2019).
  30. De Nijs, B. *et al.* Entropy-driven formation of large icosahedral colloidal clusters by spherical confinement. *Nat. Mater.* **14**, 56–60 (2015).
  31. Tanaka, S., Nogami, D., Tsuda, N. & Miyake, Y. Synthesis of highly-monodisperse spherical titania particles with diameters in the submicron range. *J. Colloid Interface Sci.* **334**, 188–194 (2009).
  32. LaMer, V. K. & Dinegar, R. H. Theory, Production and Mechanism of Formation of Monodispersed Hydrosols. *J. Am. Chem. Soc.* **72**, 4847–4854 (2002).
  33. Mao, Y., Li, Y. & Gu, N. Review: Progress in the Preparation of Iron Based Magnetic Nanoparticles for Biomedical Applications. *J. Harbin Inst. Technol. (New Ser.)* **26**, 1–18 (2019).
  34. Noorduin, W. L., Vlieg, E., Kellogg, R. M. & Kaptein, B. From Ostwald Ripening to Single Chirality. *Angew. Chemie Int. Ed.* **48**, 9600–9606 (2009).
  35. Somiya, S. Sol-Gel Process and Applications. in *Handbook of Advanced Ceramics: Materials, Applications, Processing, and Properties: Second Edition* 883–910 (Elsevier Inc., 2013). doi:10.1016/C2010-0-66261-4
  36. Barringer, E. A. & Bowen, H. K. High-purity, monodisperse TiO<sub>2</sub> powders by hydrolysis of titanium tetraethoxide. 1. Synthesis and physical properties. *Langmuir* **1**, 414–420 (2002).

37. Stöber, W., Fink, A. & Bohn, E. Controlled growth of monodisperse silica spheres in the micron size range. *J. Colloid Interface Sci.* **26**, 62–69 (1968).
38. Han, Y. *et al.* Unraveling the Growth Mechanism of Silica Particles in the Stöber Method: In Situ Seeded Growth Model. *Langmuir* **33**, 5879–5890 (2017).
39. Van Blaaderen, A., Van Geest, J. & Vrij, A. Monodisperse colloidal silica spheres from tetraalkoxysilanes: Particle formation and growth mechanism. *J. Colloid Interface Sci.* **154**, 481–501 (1992).
40. van Blaaderen, A. & Vrij, A. Synthesis and characterization of colloidal dispersions of fluorescent, monodisperse silica spheres. *Langmuir* **8**, 2921–2931 (1992).
41. Verhaegh, N. & van Blaaderen, A. Dispersions of Rhodamine-Labeled Silica Spheres: Synthesis, Characterization, and Fluorescence Confocal Scanning Laser Microscopy. *Langmuir* **10**, 1427–1438 (1994).
42. Hoitink, L. D. Studying supraparticle self-assembly. *Master Thesis* (Soft Condensed Matter group, Utrecht University, 2020).
43. Wang, J. *et al.* Free Energy Landscape of Colloidal Clusters in Spherical Confinement. *ACS Nano* **13**, 9005–9015 (2019).
44. Perez-Gonzalez, T. *et al.* Magnetite biomineralization induced by *Shewanella oneidensis*. *Geochim. Cosmochim. Acta* **74**, 967–979 (2010).
45. Sperling, M. & Gradzielski, M. Droplets, Evaporation and a Superhydrophobic Surface: Simple Tools for Guiding Colloidal Particles into Complex Materials. *Gels* **2017**, Vol. 3, Page 153, 15 (2017).
46. Bolhuis, P. & Frenkel, D. Isostructural Solid-Solid Transition in Crystalline Systems with Short Ranged Interaction. *Front. Mater. Model. Des.* 315–324 (1998). doi:10.1007/978-3-642-80478-6\_36
47. Bausch, A. R. *et al.* Grain Boundary Scars and Spherical Crystallography. *Science (80-. )*. **299**, 1716–1718 (2003).
48. Frank, F. C. & Mott, N. F. Supercooling of liquids. *Proc. R. Soc. London. Ser. A. Math. Phys. Sci.* **215**, 43–46 (1952).
49. Remiëns, S. Making supraparticles using microfluidics. *Bachelor Thesis* (Soft Condensed Matter group, Utrecht University, 2021).
50. Alberts, S. Self-assembly of amorphous titania nanoparticles into supraparticles. *Bachelor Thesis* (Soft Condensed Matter group, Utrecht University, 2020).

## 9 Laymen's summary

Nature has proven countless of times the importance of structure. An example of this are the wings of a *Morpho* butterfly. These wings are not coloured by pigmentation but by a structure resembling photonic crystals, causing reflection of light in a particular colour. This type of structural colouring is the inspiration for many new technologies such as dye-free paint.

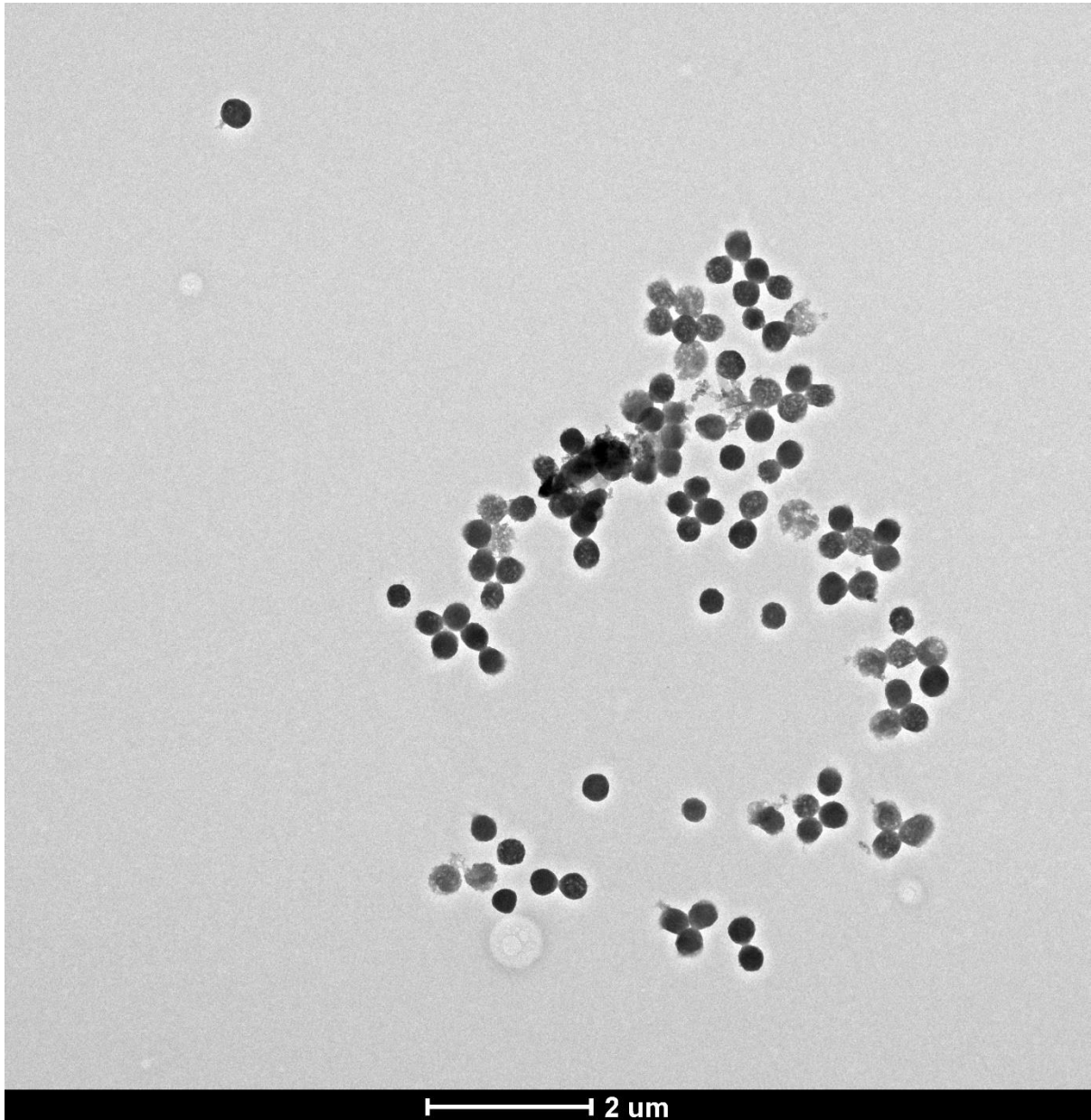
In this project we also made use of structure to manipulate light. We did this using spherical titania colloids. Colloids are particles in the range between a nanometre and a micrometre. Titania is one of the most abundant compounds on our planet and has several interesting properties such as its light scattering abilities and biocompatibility. By optimizing the structure of the titania colloids the optical properties can be enhanced, which is interesting for applications in optoelectronics, photovoltaics, photocatalysis, nanomaterials and countless of others.

One of the most powerful structures is that of a crystal, the symmetry within a crystal causes one of the strongest light interference patterns. Furthermore, crystals are often a result from natural self-assembly making the production of crystals from a bottom-up approach surprisingly easy. We made photonic crystals with our titania colloids through evaporation-induced self-assembly. Which means that we forced the self-assembly of the colloids by gradually confining their space. The result of this are spherical structures which we call *supraparticles*. The supraparticles come in different shapes and sizes, but the most crystalline, and thus structured, ones have the most optical potency. To increase the ability of the colloids to self-assemble into their most favourable and highly structured state, it was important for the colloids to all have the same shape and size. We succeeded in making stable spherical colloids consisting of a combination of titania and silica that only differed 3% from each other. Using these colloids we were able to create onion-shaped, the name used for structured layers of colloids on top of each other, supraparticles as well as highly structured icosahedral supraparticles, showing five-fold symmetry, with strong iridescent features.

However, not all supraparticles were as beautiful as the others. This is mainly because a lot of the self-assembly process is still unclear and the parameters used in the experiments could probably be optimized a lot. If we have more control over the formation of the supraparticles, it would be easier to synthesize them in bulk in the future. Eventually, because of their strong optical properties they could become very interesting for numerous applications in the fields of nanophotonics and photocatalysis or potentially replace dyes by using them for structural colouring.

## 10 Appendices

### 10.1 Titania colloids dissolved in ethanol



**Appendix figure 1:** Titania colloids after dispersing in ethanol (24h), colloids are clearly dissolving and losing their monodispersity and circular properties.

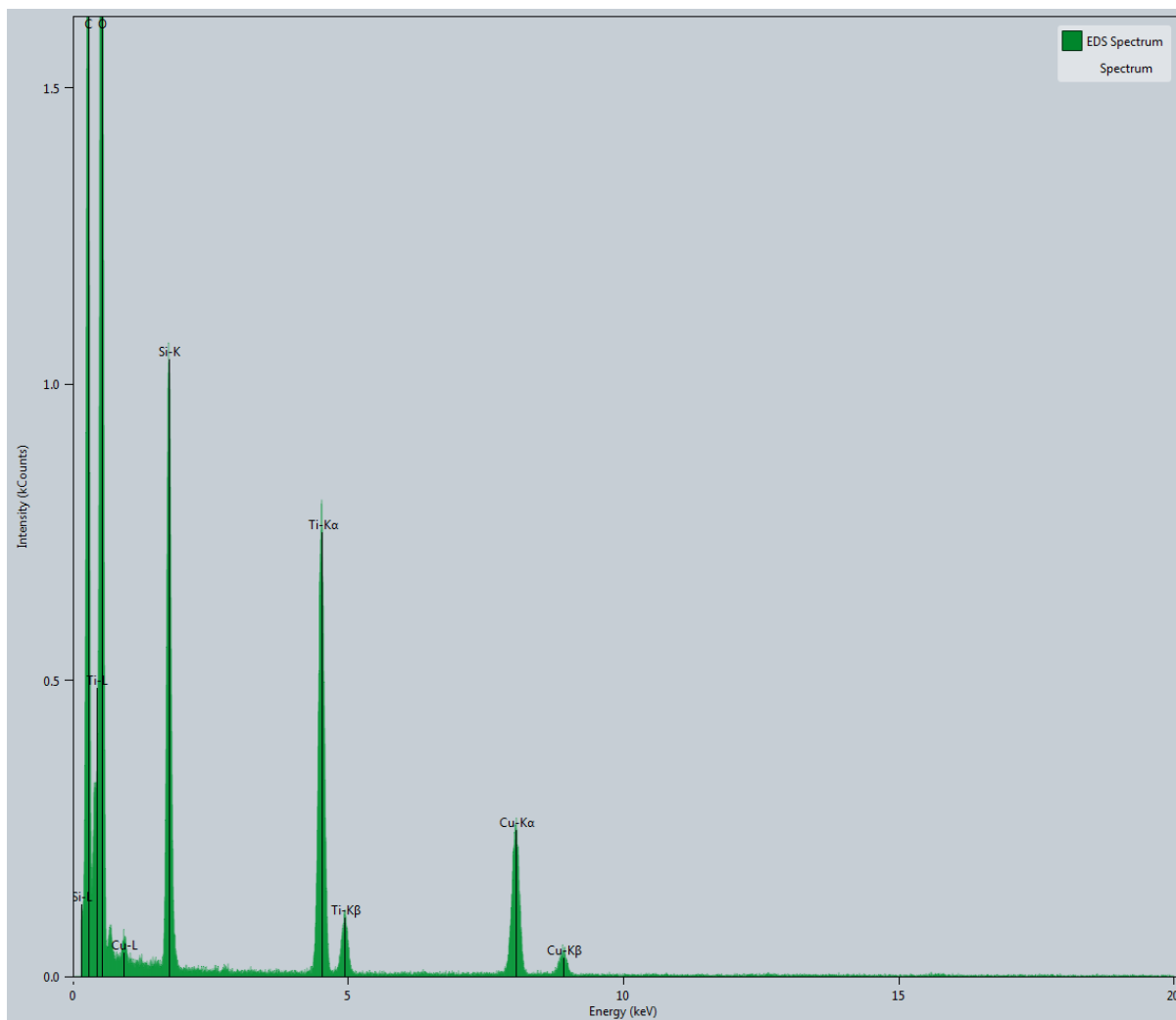
## 10.2 EDX titania-silica composites

Appendix table 1: TiO<sub>2</sub>-SiO<sub>2</sub> EDX-EDS Spectrum-Composition

Z	Element	Family	Net intensity	Net background	K-factor	Absorption correction	Atomic fraction	Mass fraction	Fit error
-	-	-	counts	counts	-	-	%	%	%
6	C	K	2.46E+04	2.57E+02	1.00E+00	1.00E+00	4.44E+01	2.80E+01	2.53E+00
8	O	K	3.81E+04	3.63E+02	7.01E-01	1.00E+00	3.62E+01	3.04E+01	3.29E-01
14	Si	K	1.95E+04	6.05E+02	6.21E-01	1.00E+00	9.33E+00	1.38E+01	8.12E-02
22	Ti	K	2.17E+04	7.41E+02	7.22E-01	1.00E+00	7.08E+00	1.78E+01	7.35E-02
29	Cu	K	8.94E+03	5.50E+02	9.75E-01	1.00E+00	2.98E+00	9.94E+00	1.89E-01

Appendix table 2: TiO<sub>2</sub>-SiO<sub>2</sub> EDX-EDS Spectrum-Lines

Line identifier	Energy level	Intensity	Chi-Rho-Tau absorption	K-factor
-	eV	counts	-	-
<i>C-Ka1</i>	2.80E+02	2.46E+04	0.00E+00	1.00E+00
<i>O-Ka1</i>	5.24E+02	3.81E+04	0.00E+00	7.01E-01
<i>Si-Ka1</i>	1.74E+03	1.87E+04	0.00E+00	6.21E-01
<i>Si-Kb1</i>	1.83E+03	7.49E+02	0.00E+00	6.21E-01
<i>Si-Lb4</i>	1.55E+02	1.63E+03	0.00E+00	4.30E+01
<i>Ti-Ka1</i>	4.51E+03	1.26E+04	0.00E+00	7.22E-01
<i>Ti-Ka2</i>	4.50E+03	6.32E+03	0.00E+00	7.22E-01
<i>Ti-Kb1</i>	4.93E+03	2.58E+03	0.00E+00	7.22E-01
<i>Ti-La1</i>	4.50E+02	2.11E+03	0.00E+00	2.54E+00
<i>Ti-La2</i>	4.56E+02	2.11E+02	0.00E+00	2.54E+00
<i>Ti-Lb1</i>	4.62E+02	4.23E+02	0.00E+00	2.58E+00
<i>Ti-Lb3</i>	5.30E+02	8.46E+01	0.00E+00	3.22E+00
<i>Ti-Lb4</i>	5.26E+02	8.46E+01	0.00E+00	3.22E+00
<i>Ti-Ll</i>	3.97E+02	2.96E+03	0.00E+00	2.54E+00
<i>Ti-Ln</i>	4.03E+02	1.16E+03	0.00E+00	2.58E+00
<i>Cu-Ka1</i>	8.05E+03	5.24E+03	0.00E+00	9.75E-01
<i>Cu-Ka2</i>	8.03E+03	2.62E+03	0.00E+00	9.75E-01
<i>Cu-Kb1</i>	8.91E+03	1.06E+03	0.00E+00	9.75E-01
<i>Cu-La1</i>	9.30E+02	4.51E+02	0.00E+00	1.36E+00
<i>Cu-La2</i>	9.29E+02	4.51E+01	0.00E+00	1.36E+00
<i>Cu-Lb1</i>	9.49E+02	8.12E+01	0.00E+00	1.39E+00
<i>Cu-Lb3</i>	1.02E+03	4.51E+00	0.00E+00	1.64E+00
<i>Cu-Lb4</i>	1.02E+03	4.51E+00	0.00E+00	1.64E+00
<i>Cu-Ll</i>	8.12E+02	4.96E+01	0.00E+00	1.36E+00
<i>Cu-Ln</i>	8.31E+02	2.25E+01	0.00E+00	1.39E+00



Appendix figure 2: EDX spectrum titania-silica composites



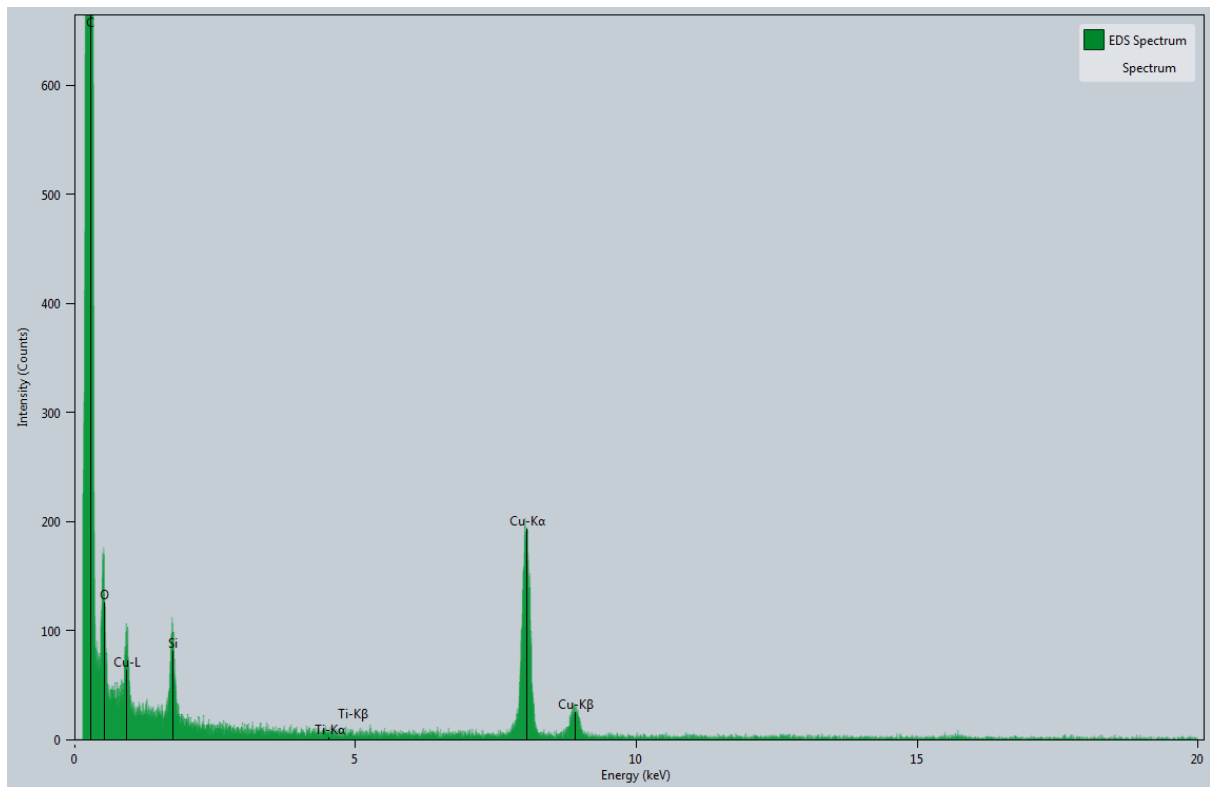
### 10.3 EDX OTMOS coated titania-silica composites

Appendix table 3: TiO<sub>2</sub>-SiO<sub>2</sub>-C18 EDX-EDS Spectrum-Composition

Z	Element	Family	Net intensity counts	Net background counts	K-factor	Absorption correction	Atomic fraction %	Mass fraction %	Fit error %
-	-	-	-	-	-	-	-	-	-
6	C	K	2.04E+05	4.13E+02	1.00E+00	1.00E+00	9.87E+01	9.57E+01	2.00E+00
8	O	K	1.87E+03	5.82E+02	7.01E-01	1.00E+00	4.76E-01	6.15E-01	1.92E+00
14	Si	K	1.57E+03	6.52E+02	6.21E-01	1.00E+00	2.01E-01	4.56E-01	7.33E-01
22	Ti	K	6.47E+01	7.96E+02	7.22E-01	1.00E+00	5.66E-03	2.19E-02	9.12E+00
29	Cu	K	6.98E+03	6.90E+02	9.75E-01	1.00E+00	6.22E-01	3.19E+00	1.96E-01

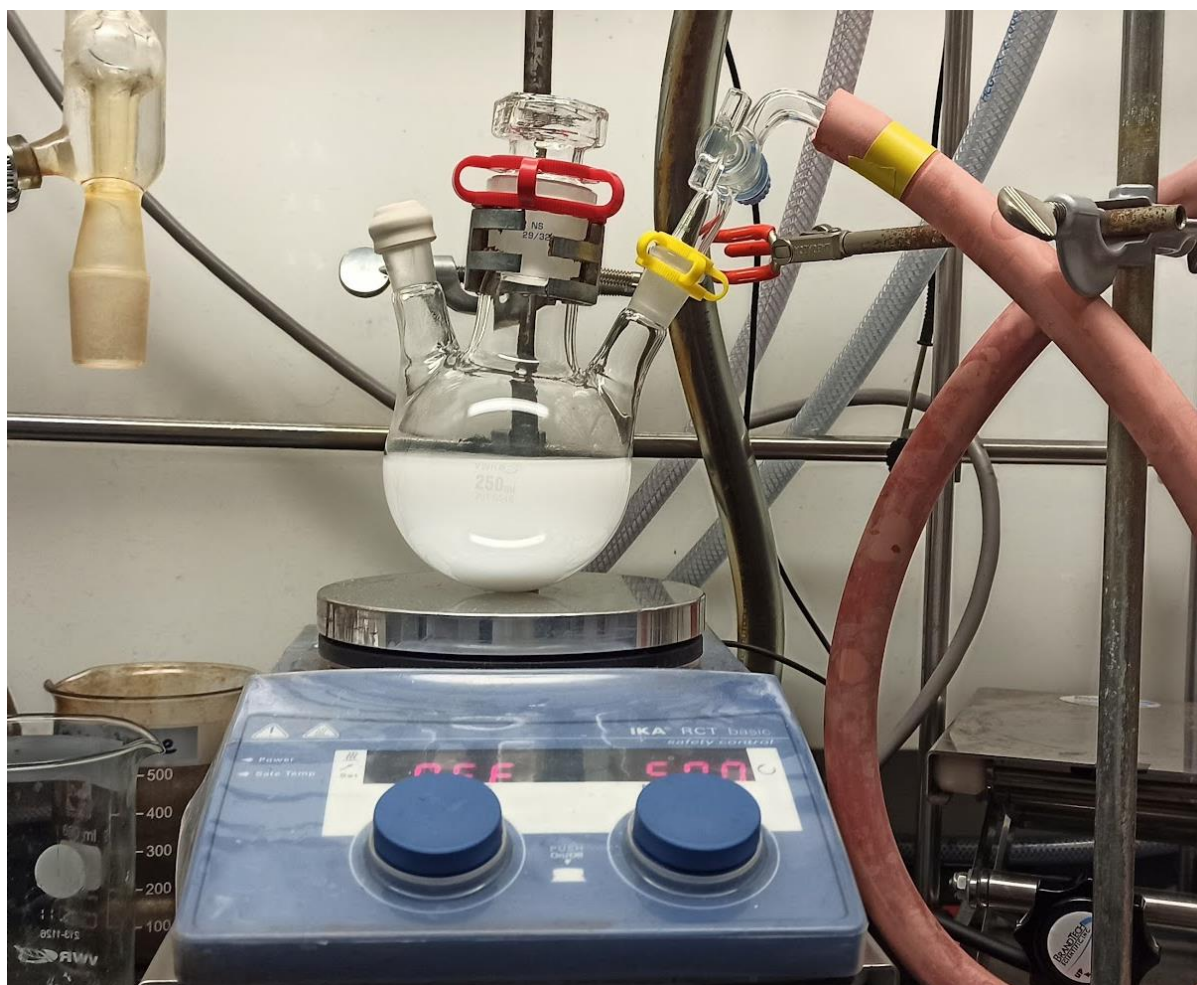
Appendix table 4: TiO<sub>2</sub>-SiO<sub>2</sub>-C18 EDX-EDS Spectrum-Lines

Line identifier	Energy level eV	Intensity counts	Chi-Rho-Tau absorption	K-factor
-	eV	counts	-	-
C-Ka1	2.80E+02	2.04E+05	0.00E+00	1.00E+00
O-Ka1	5.24E+02	1.87E+03	0.00E+00	7.01E-01
Si-Ka1	1.74E+03	1.51E+03	0.00E+00	6.21E-01
Ti-Ka1	4.51E+03	3.78E+01	0.00E+00	7.22E-01
Ti-Ka2	4.50E+03	1.89E+01	0.00E+00	7.22E-01
Ti-Kb1	4.93E+03	7.70E+00	0.00E+00	7.22E-01
Ti-La1	4.50E+02	0.00E+00	0.00E+00	2.54E+00
Ti-La2	4.56E+02	0.00E+00	0.00E+00	2.54E+00
Ti-Lb1	4.62E+02	0.00E+00	0.00E+00	2.58E+00
Ti-Ll	3.97E+02	0.00E+00	0.00E+00	2.54E+00
Ti-Ln	4.03E+02	0.00E+00	0.00E+00	2.58E+00
Cu-Ka1	8.05E+03	4.09E+03	0.00E+00	9.75E-01
Cu-Ka2	8.03E+03	2.05E+03	0.00E+00	9.75E-01
Cu-Kb1	8.91E+03	8.31E+02	0.00E+00	9.75E-01
Cu-La1	9.30E+02	7.43E+02	0.00E+00	1.36E+00
Cu-La2	9.29E+02	7.43E+01	0.00E+00	1.36E+00
Cu-Lb1	9.49E+02	1.34E+02	0.00E+00	1.39E+00
Cu-Ll	8.12E+02	8.17E+01	0.00E+00	1.36E+00

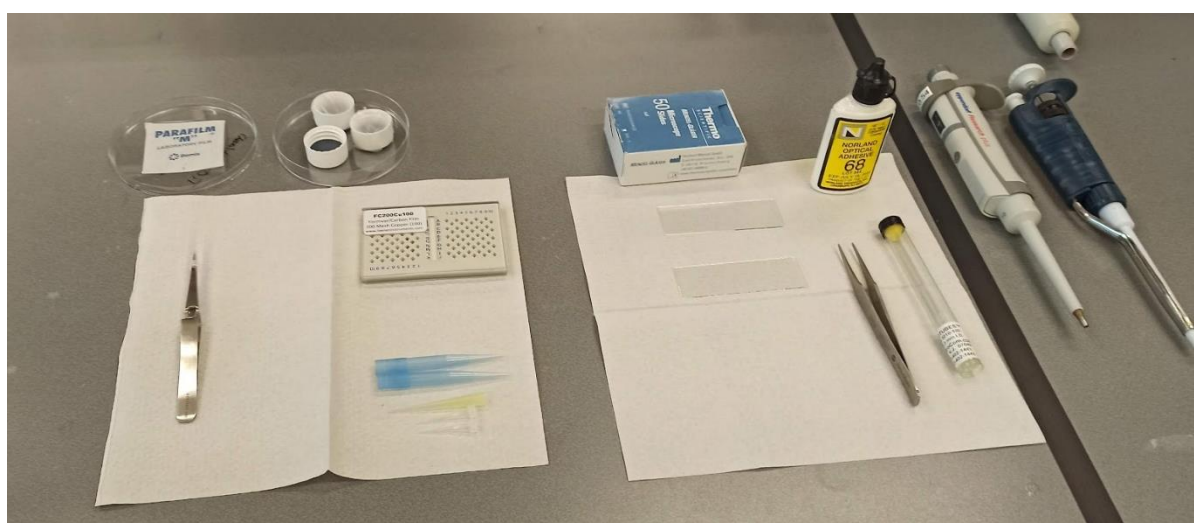


Appendix figure 3: EDX spectrum OTMOS coated titania-silica composites

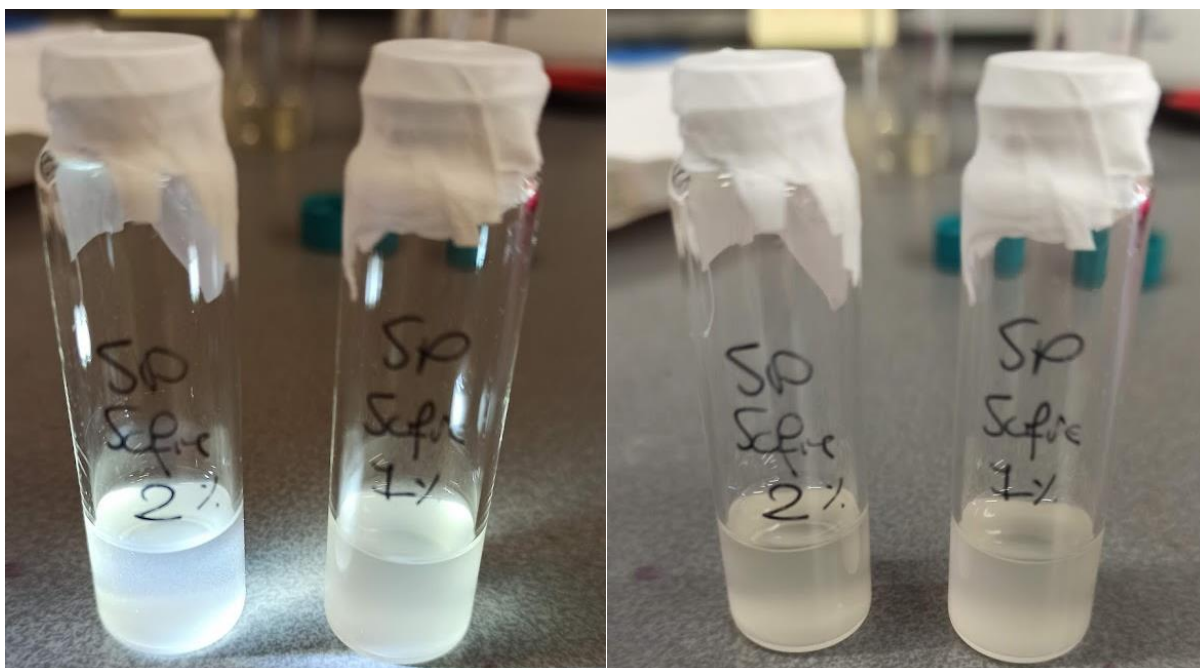
## 10.4 Synthesis Set-Ups



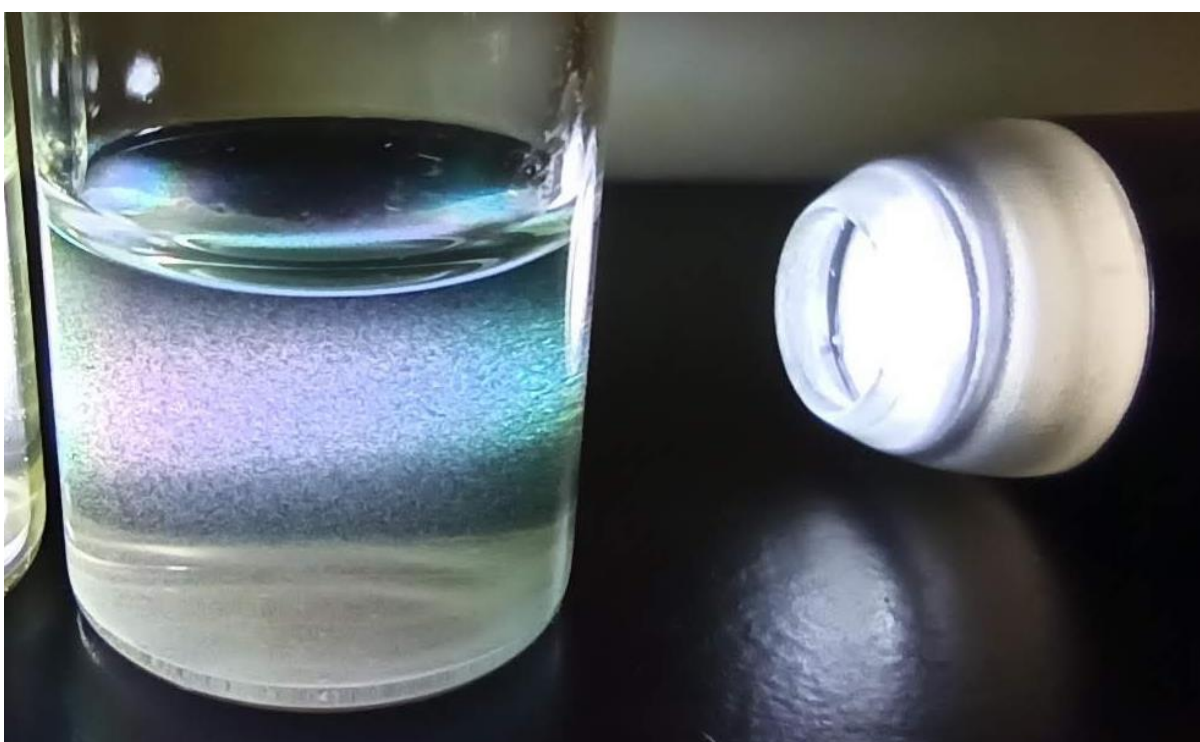
Appendix figure 4: Titania colloid synthesis sol-gel method set-up



Appendix figure 5: TEM sample preparation tools (left) and confocal sample preparation tools (right)



**Appendix figure 6:** Supraparticle synthesis start (before drying). Illuminated with a broad spectrum pen light (left) and natural light (right).



**Appendix figure 7:** Supraparticle synthesis finish (after drying). Illuminated with a broad spectrum pen light, showing rainbow colours.

## 10.5 Polydispersity Python code from Maarten Bransen

```
# -*- coding: utf-8 -*-
"""
Maarten Bransen

Last updated: 14/01/2020
"""
#=====
# %%IMPORTS
#=====

import cv2
import numpy as np
import matplotlib.pyplot as plt
import pandas as pd
from scm_electron_microscopes import tecnai
from matplotlib.patches import Ellipse

#=====
# %%DEFINITIONS
#=====

def
calculate_contour_properties(segmentim,particles,functions,parallelize_cutoff
=200):
    """
    Calculates contour for each particle and applies functions to them
    to
    determine properties.

    Parameters
    -----
    segmentim : 2d numpy array
        2d array with int pixel values corresponding to the index label
    of the
        contour they correspond to. As output by opencv watershed
    particles : set
        set of index labels to consider in segmentim.
    functions : dict of callable
        dict of functions. Keys will be used for column headers, items
    must be
        functions taking only a contour as argument, the returned item
    is used
        as value for the DataFrame.
    parallelize_cutoff : int, optional
        minimum number of particles to use the parallelized countour
    with
        calculation, below this value a normal sequential loop is used

        less overhead. The default is 200.

    Returns
    -----
    result : pandas DataFrame
```

```

        table with a row for each particle and a column for each of the
        calculated properties from the dict of functions

"""
n = len(particles)
import time
t = time.time()

#when there are not many particles, run in a conventional loop
if n < parallelize_cutoff:
    print('low particle count, using single core processing')
    result = []
    for i,p in enumerate(particles):
        result.append(_cont_props(p,segmentim,functions))
        print('\rcalculating properties, {:d}%
done'.format(int(i/(n-1)*100)),end='',flush=True)

    result =
pd.DataFrame(data=result).dropna(axis=0).set_index('particle')
    print('')

#otherwise, paralellize the computation to gain speed
else:
    import multiprocessing as mp
    from itertools import repeat

    cores = mp.cpu_count()
    print('initializing parallel processing on {} processor
cores'.format(cores))

    #create processor pool and map cont_props function in random
order
    pool = mp.Pool(cores)
    result =
pool.starmap_async(_cont_props,zip(particles,repeat(segmentim),repeat(f
unctions)))

    #print output every 0.1 s and wait until result is ready
chunksize = result._chunksize
    while not result.ready():
        i = max([int((n-result._number_left*chunksize)/n*100),0])
        print('\rcalculating properties, {:d}%
done'.format(i),end='',flush=True)
        time.sleep(0.1)

    #finish parallel processes, wait for everything to complete
pool.close()
pool.join()
    print('\rcalculating properties, 100% done',flush=True)

    result =
pd.DataFrame(data=result.get()).dropna(axis=0).set_index('particle')

#print calculation time
print('calculation took {:.2f} s'.format(time.time()-t))
return result

```

```

def _cont_props(p, segmentim, functions):
    """
    wrapper function for calculate_contour_properties to enable
    parallelization
    """

    #find contour
    contour =
cv2.findContours(np.ndarray.astype(segmentim==p, np.uint8), cv2.RETR_EXTE
RNAL, cv2.CHAIN_APPROX_NONE)

    #opencv changed return order since version 4
if int(cv2.__version__[0]) >= 4:
        contour = contour[0][0]
else:
        contour = contour[1][0]

    #calculate properties and append
if len(contour)>5:
        props = {key:function(contour) for key,function in
functions.items()}

else:
        props = {key:np.nan for key in functions.keys()}

    props['particle'] = p
    return props

def circularity(contour):
    """calculates circularity of contour"""
    return
4*np.pi*cv2.contourArea(contour)/cv2.arcLength(contour, True)**2

class contourclicker:
    """
    Opens figure with ellipses highlighted and removes them from data
    if
    clicked. Requires, reads and alters global variables!

    Note: the class instance must be assigned to a global variable or
    else it
    is garbage collected and does not work.
    """
    def __init__(self, figure, axes, contourmap, properties):
        """
        initialize class and create the figure
        """
        #assign attributes
        self.fig = figure
        self.ax = axes
        contourmap[np.isin(contourmap, properties.index, invert=True)] =
0

        self.map = contourmap
        self.map_original = self.map.copy()
        self.properties = properties
        self.properties_original = self.properties.copy()

```

```

#connect events to figure handle
figure.canvas.mpl_connect('button_press_event', self.onclick)
figure.canvas.mpl_connect('key_press_event', self.onkey)
figure.canvas.mpl_connect('key_release_event',
self.onkeyrelease)
    self.alt_on = False

    self.print_help()
    self.draw_all()

def onclick(self, event):
    if event.button == 1 and self.alt_on and \
        type(event.xdata) != type(None) and
type(event.xdata) !=type(None):
        p = self.map[int(event.ydata), int(event.xdata)]
        if p != 0:
            print('removing particle',p)

self.ax.artists[self.properties.index.get_loc(p)].remove()
    self.properties = self.properties.drop([p])
    self.map[self.map==p] = 0
    self.fig.canvas.draw()
    #self.draw_all()

def onkey(self, event):
    if event.key == 'alt+s':
        self.save_global()
        self.save_file()
    elif event.key == 'alt+r':
        self.reset()
    elif event.key == 'alt+h':
        self.print_help()
    elif event.key == 'alt+c':
        self.save_global()

    if event.key == 'alt':
        self.alt_on = True

def onkeyrelease(self, event):
    if event.key == 'alt':
        self.alt_on = False

def draw_all(self):
    """update the figure"""
    if len(self.ax.artists)!=0:
        [p.remove() for p in reversed(self.ax.artists)]

[self.ax.add_artist(Ellipse(i[0],i[1][0],i[1][1],i[2],ec='r',fc='none')
) for i in self.properties['ellipse']]
    self.fig.canvas.draw()

def reset(self):
    """restart from beginning"""
    self.properties = self.properties_original.copy()
    self.map = self.map_original.copy()

```



```

self.update()
print('Resetting data')

def save_global(self):
    """confirms new datasets to global variables and alters reset
state"""
    global properties, results
    properties = self.properties
    results['properties'] = self.properties
    global statistics
    statistics = statistics_dict(properties, unit)
    self.properties_original = self.properties.copy()
    self.map_original = self.map.copy()
    plot_histograms(properties, unit, statistics)
    print('Selection saved to new reset state')

def save_file(self):
    """save data to files"""

    write_textfile(data.filename[:-4]+'_statistics.txt', statistics)
    write_settings(data.filename[:-4]+'_settings.txt', settings)

    import pickle
    with open(data.filename[:-4]+'_data.pkl', 'wb') as f:
        pickle.dump(results, f)

def print_help(self):
    """print list of options"""
    print('\n ----- ')
    print(' |                               OPTIONS                               | ')
    print(' |                               | ')
    print(' | - alt+click on a particle to remove it | ')
    print(' | - alt+r to reset particles | ')
    print(' | - alt+c to commit current state to reset state | ')
    print(' | - alt+s to save current state to file | ')
    print(' | - alt+h to display help/options | ')
    print(' | ----- \n')

def dilate_disc(binary, rad):
    """
    performs image dilation with a disc kernel of radius 'rad'
    """
    y, x = np.ogrid[-np.ceil(rad): np.ceil(rad)+1, -np.ceil(rad):
np.ceil(rad)+1]
    kernel = x**2+y**2 <= rad**2
    return cv2.dilate(binary, np.ndarray.astype(kernel, np.uint8))

def filter_dataframe(properties, filters = []):
    """
    removes particles which fall outside of range

    Parameters
    -----
    properties : pandas DataFrame
        properties for each particle (dataframe index)
    filters : list of tuples of form ('column', min, max)
        properties and min/max values to filter by.

```

```

Returns
-----
properties : pandas DataFrame
    the property dataframe with filtered elements removed

"""
for f in filters:
    if f[1] != None:
        properties = properties.loc[properties[f[0]]>=f[1]]
    if f[2] != None:
        properties = properties.loc[properties[f[0]]<=f[2]]

return properties

def fit_ellipse(contour,x=2):
    """fits contour with ellipse, adds x pixels to diameter"""
    el = cv2.fitEllipse(contour)
    return (el[0],(el[1][0]+x,el[1][1]+x),el[2])

def plot_histograms(properties,unit,statistics,nbins=25,loc=[2,1]):
    """plot histogram of diameter and aspect ratio"""
    from matplotlib.offsetbox import AnchoredText
    #from general_functions import style_plot

    #close figures if they exist already
    plt.close('Diameter')
    plt.close('Aspect ratio')

    with plt.rc_context({}):#style_plot():
        #diameter
        plt.figure('Diameter')
        plt.gcf().set_size_inches(4,3)
        plt.hist(properties['diameter'],nbins,fc=[0.2, 0.4470,
0.8708],ec='k')
        plt.xlabel('diameter ('+unit+')')
        plt.ylabel('occurrence')
        text = 'N:\t{\nD:\t{:.3g}\t{:.2g} '.format(
            statistics['particles'][0],
            statistics['diameter mean'][0],
            statistics['diameter  $\sigma$ '][0]).expandtabs(4) + unit

plt.gca().add_artist(AnchoredText(text,loc=loc[0],prop={'fontsize':10})
)

    plt.tight_layout()

    #aspect ratio
    plt.figure('Aspect ratio')
    plt.gcf().set_size_inches(4,3)
    plt.hist(properties['aspect ratio'],nbins,fc=[0.2, 0.4470,
0.8708],ec='k')
    plt.xlabel('aspect ratio')
    plt.ylabel('occurrence')
    text = 'N:\t{\nAR:\t{:.2g}\t{:.1g} '.format(
        statistics['particles'][0],
        statistics['aspect ratio mean'][0],
        statistics['aspect ratio  $\sigma$ '][0]).expandtabs(4)

```

```

plt.gca().add_artist(AnchoredText(text,loc=loc[1],prop={'fontsize':10})
)
plt.tight_layout()

def load_measurement_results(files):
    """loads dataframes from pickled data and concatenates them"""
    import pickle

    #load file
    properties = []
    for file in files:
        print(file)
        with open(file,'rb') as f:
            data = pickle.load(f)
        #extract dataframe, add filename as column
        p = data['properties']
        p['image'] = [file[:-9]+'.tif']*len(p)
        #convert unit to nm if needed
        if data['unit'] == 'µm':
            p['diameter'] = p['diameter']*1e3
        #append to list of dataframes
        properties.append(p)

    if len(files) > 1:
        return pd.concat(properties)
    else:
        return properties[0]

def remove_border_contours(segmentim,ignore={-1,0},setval=0):
    """Removes all contours on the image border"""

    #find set of all values which occur 0 or 1 pixels from border
    t = set(segmentim[:2].ravel())
    b = set(segmentim[-2:].ravel())
    l = set(segmentim[:,2].ravel())
    r = set(segmentim[:, -2:].ravel())

    #join and remove items to be ignored
    bordervals = (l | r | t | b) - ignore

    #set the border contours to setval in image
    segmentim[np.isin(segmentim,list(bordervals))] = setval
    return segmentim

def saveprompt(question="Save/overwrite results? 1=yes, 0=no. "):
    """
    aks user to save, returns boolean
    """
    try:
        savefile = int(input(question))
    except ValueError:
        savefile = 0
    if savefile>1 or savefile<0:
        savefile = 0
    if savefile==1:
        print("saving data")

```

```

        save = True
    else:
        print("not saving data")
        save = False
    return save

def set_figure_fullsize (figure):
    """
    Set a spyder figure window to fullsize automatically. Platform and
    figure manager dependent.

    @dependencies:
        from matplotlib import pyplot as plt

    @parameters:
        figure:      matplotlib.pyplot.figure handle
    """
    activefig = plt.gcf()
    plt.figure(figure.number)
    mngr = plt.get_current_fig_manager()
    mngr.window.showMaximized()
    plt.figure(activefig.number)#set current figure back

def statistics_dict (properties,unit):
    """build a dictionary with mean and std of properties"""
    statistics = {
        'particles':(len(properties),''),
        'diameter mean':(properties['diameter'].mean(),unit),
        'diameter  $\sigma$ ':(properties['diameter'].std(),unit),
        'diameter rel.
 $\sigma$ ':(100*properties['diameter'].std()/properties['diameter'].mean(),'%')
    ,
        'aspect ratio mean':(properties['aspect ratio'].mean(),''),
        'aspect ratio  $\sigma$ ':(properties['aspect ratio'].std(),''),
        'aspect ratio rel.  $\sigma$ ':(100*properties['aspect
ratio'].std()/properties['aspect ratio'].mean(),'%'),
        #'circularity mean':(properties['circularity'].mean(),''),
        #'circularity  $\sigma$ ':(properties['circularity'].std(),''),
        #'circularity rel.
 $\sigma$ ':(100*properties['circularity'].std()/properties['circularity'].mean(
),'%')
    }
    #print formatted output
    print('* particles:',statistics['particles'][0])
    print('* diameter:\t {:.4g}±{:.2f} ({:.3g}%)'.format(
        statistics['diameter mean'][0],
        statistics['diameter  $\sigma$ '][0],
        statistics['diameter rel.  $\sigma$ '][0]
    ) + unit)
    print('* aspect ratio:\t {:.4g}±{:.2g} ({:.3g}%)'.format(
        statistics['aspect ratio mean'][0],
        statistics['aspect ratio  $\sigma$ '][0],
        statistics['aspect ratio rel.  $\sigma$ '][0]
    )
    #print('* circularity:\t {:.3g}±{:.1g}
({:.2g}%)'.format(statistics['circularity

```

```

mean'] [0], statistics['circularity  $\sigma$ '] [0], statistics['circularity rel.
 $\sigma$ '] [0]))

    return statistics

def write_settings(filename, params):
    """
    stores parameter names and values in text file

    @dependencies:
        import io

    @parameters
        params: dictionary of name:value
        filename: string.txt

    @returns:
        none, but stores file to disc
    """
    import io
    with io.open(filename, 'w', encoding="utf-8") as file:
        for key, val in params.items():
            file.write(str(key)+' = '+str(val)+'\n')
    print("input parameters saved in", filename)

def write_textfile(filename, params):
    """
    stores parameter names and values in text file

    @parameters
        params: dictionary of name:value
        filename: string.txt
    """
    #find longest string in columns
    keylen = len(max(params, key=len))
    unitlen = max([len(val[1]) for _, val in params.items()])

    import io
    with io.open(filename, 'w', encoding="utf-8") as file:
        #write header line
        file.write('PROPERTY\t'.expandtabs(keylen+4)+'UNIT\t'.expandtabs(unitlen+4)+'VALUE')
        #write data lines
        for key, val in params.items():
            line =
            (str(key)+'\t').expandtabs(keylen+4)+(val[1]+'\t').expandtabs(unitlen+4)
            +str(val[0])
            file.write('\n'+line)

        print("results saved in", filename)

#=====
# %%INPUT

```

```

=====
#
# filename:          str containing the name of the file to load in
current WD
#
# blursize:         size (in pixels) of gaussian kernal to use for
smoothing of
#
#                   image used for thresholding
#
# dilate:           diameter (in pixels) of disc kernal to expand
features by
#
#                   for background guess. Increase if contours are
smaller than
#
#                   particles, decrease if bg between particles is
lost.
#
# thresholdfactor: factor to multiply automatic threshold with. Higher
value
#
#                   leads to smaller features / more background in
binary im.
#
# distancethresh:  fraction of maximum value in distance transform to
use as
#
#                   threshold value. (between 0 and 1). Increase if
particles
#
#                   merge together, decrease if small particles are no
longer
#
#                   found.
#
# mindiam,maxdiam: cut-off values (in data units, inclusive) for
filtering
#
#                   particles based on diameter. Use None,None for no
filtering
#
# minar,maxar:     cut-off values (inclusive) for filtering based on
AR. For
#
#                   approximately spherical particles recommended to
set maxar
#
#                   to 1.5 to filter out merged particles.

#file (inc. extension)
file = '5 '
#preprocessing
blursize = 5
dilate = 20
thresholdfactor = 1
distancethresh = 0.4
watershedblur = 1

#filtering results
mindiam,maxdiam = None, None
minar,maxar = None, 1.3

=====
# %%RUN THE CODE

```

```

=====
#needed for parallel processing
if __name__ == '__main__':

    #close all open figures
    plt.close('all')

    #store settings
    settings = {
        'file':file,
        'blursize':blursize,
        'dilate':dilate,
        'thresholdfactor':thresholdfactor,
        'distancethresh':distancethresh,
        'watershedblur':watershedblur,
        'mindiam':mindiam,
        'maxdiam':maxdiam,
        'minar':minar,
        'maxar':maxar
    }

    #import datasorry th
    data = tecnai(file)
    im = 255 - data.image
    pixelsize,unit = data.get_pixelsize(debug=False)
    if unit == 'µm':
        unit = 'nm'
        pixelsize = pixelsize * 1000

    #blur
    if blursize == 0:
        blur = im.copy()
    else:
        blur = cv2.blur(im, (blursize,blursize))

    #blur
    if watershedblur == 0:
        wsblurim = im.copy()
    else:
        wsblurim = cv2.blur(im, (watershedblur,watershedblur))

    print('thresholding')
    #create binary
    thresh,_ =
cv2.threshold(blur,0,255,cv2.THRESH_BINARY+cv2.THRESH_OTSU)
    _,binary =
cv2.threshold(blur,thresh*thresholdfactor,255,cv2.THRESH_BINARY)

    #dilate with circle kernel
    bg = dilate_disc(binary,dilate/2)

    #find trial locations of particles with distance transform
    (foreground)
    distance =
np.array(cv2.distanceTransform(binary,cv2.DIST_L2,5),dtype=np.uint8)

```

```

_, fg =
cv2.threshold(distance, distancethresh*distance.max(), 255, cv2.THRESH_BIN
ARY)

#boundary region between background and trial particles
boundary = bg-fg

print('performing watershed')
#find boundary region and label it 0, bg is 1, rest is particles
_, trialparticles = cv2.connectedComponents(fg)
trialparticles += 1
trialparticles[boundary==255] = 0

#apply watershed
segment = cv2.watershed(cv2.cvtColor(wsblurim,
cv2.COLOR_GRAY2BGR), trialparticles)-1
segment[segment==-2] = -1
n = np.amax(segment)

#segmentation result, show contours with red line
resultim = cv2.cvtColor(255-wsblurim, cv2.COLOR_GRAY2RGB)
resultim[cv2.dilate(np.ndarray.astype(segment==
1, np.uint8), np.ones((2, 2), np.uint8))==1] = [255, 0, 0]

#plot a figure with all the different steps in the segmentation
fig, ax = plt.subplots(2, 3, sharex=True, sharey=True)
fig.canvas.set_window_title('Debugging')
set_figure_fullsize(fig)
[a.axis('off') for a in ax.ravel()]
ax[0, 0].imshow(blur, cmap='Greys')
ax[0, 0].set_title('blurring')
ax[0, 1].imshow(distance, cmap='Greys_r')
ax[0, 1].set_title('distance transform')
ax[0, 2].imshow(bg, cmap='Greys_r')
ax[0, 2].set_title('dilation')
ax[1, 0].imshow(binary, cmap='Greys_r')
ax[1, 0].set_title('thresholding')
ax[1, 1].imshow(fg, cmap='Greys_r')
ax[1, 1].set_title('particles')
ax[1, 2].imshow(resultim)
ax[1, 2].set_title('segmentation')
fig.tight_layout()

#remove anything touching the image border
segment = remove_border_contours(segment)
particles = set(segment.ravel()) - {-1, 0}
n = len(particles)
print('initial particles: {}'.format(n))

#calculate ellipses and other properties
functions = {'ellipse': fit_ellipse}#, 'circularity': circularity}
properties =
calculate_contour_properties(segment, particles, functions)
properties = properties.loc[properties['ellipse'].apply(lambda i:
i[1][0]>0)]

#obtain further statistics from ellipses

```



```

    properties['diameter'] = properties['ellipse'].apply(lambda i:
(i[1][0]*i[1][1])**0.5*pixelsize)
    properties['aspect ratio'] = properties['ellipse'].apply(lambda i:
i[1][1]/i[1][0])

    #remove outliers based on criteria
    properties =
filter_dataframe(properties, [('diameter',mindiam,maxdiam), ('aspect
ratio',minar,maxar)])

    #scale diameters and store results
    n = len(properties)
    results = {
        'pixelsize':pixelsize,
        'unit':unit,
        'properties':properties
    }

    #plot interactively
    fig = plt.figure('Interactive inspection window')
    ax2 = fig.add_subplot(111,sharex=ax[0,0],sharey=ax[0,0])
    set_figure_fullsize(fig)
    ax2.imshow(im,cmap='Greys')
    plt.axis('off')
    plt.tight_layout()

    #make interactive
    interactive_figure = contourclicker(fig,ax2,segment,properties)

    #plot some histograms
    statistics = statistics_dict(properties,unit=unit)
    plot_histograms(properties,unit,statistics)

import sys
    sys.exit()

=====
=====
# %%COMBINE MULTIPLE DATASETS
=====
=====

files = '*.pkl' #glob string
load_saved_data = True

if __name__ != '__main__':
    load_saved_data = False

if load_saved_data:
    import glob
    files = glob.glob(files)
    properties = load_measurement_results(files)
    properties = filter_dataframe(properties, [('diameter', None, None),
('aspect ratio', None, None)]
    unit = 'nm'
    statistics = statistics_dict(properties,unit=unit)
    plot_histograms(properties,unit,statistics,nbins=50)
    write_textfile(files[0][:-12]+'_statistics.txt',statistics)

```

```

#=====
=====
# %%COMBINE MULTIPLE SAMPLES
#=====
=====

files =
['MB145_rewashed_bott*_data.pkl', 'MB145_rewashed_mid*_data.pkl', 'MB145_
rewashed_top*_data.pkl'] #glob string
legendnames = ['A', 'B', 'C']
load_saved_data = True

if __name__ != '__main__':
    load_saved_data = False

if load_saved_data:
    import glob
    from matplotlib.colors import to_rgb

    plt.close('Diameters')
    fig = plt.figure('Diameters')
    ax = fig.add_subplot(111)
    fig.set_size_inches(4,3)

    for name, file in zip(legendnames, files):
        samplefiles = glob.glob(file, recursive=True)
        properties = load_measurement_results(samplefiles)
        properties =
filter_dataframe(properties, [('diameter', None, None), ('aspect
ratio', None, None)]
        n = len(properties)
        color =
list(to_rgb(next(ax._get_patches_for_fill.prop_cycler)["color"]))
        ax.hist(properties['diameter'], weights=np.ones(n)*100/n,
bins=50, label=name, fc=color+[0.5], ec='k')

        plt.xlabel('diameter (nm)')
        plt.ylabel('relative occurrence (%)')
        plt.legend(fontsize=9, fancybox=False, frameon=False)
        plt.tight_layout()

```